THEORY FOR THE ELECTRONIC STRUCTURE AT THE SURFACE OF TRANSITION METAL ALLOYS

Thesis submitted for the Degree
DOCTOR RERUM NATURALIUM
in the Fachbereich Physik
of the Freie Universität Berlin

by

José Luis Morán-López
from Charcas, SLP, México

1977

THEORY FOR THE ELECTRONIC STRUCTURE AT THE SURFACE OF TRANSITION METAL ALLOYS

Thesis submitted for the Degree
DOCTOR RERUM NATURALIUM
in the Fachbereich Physik
of the Freie Universität Berlin

by

José Luis Morán-López
from Charcas, SLP, México

UNIV.
LEIDEN
BIBL.

Theorie der elektronischen Struktur an Oberflächen von Übergangsmetall-Legierungen

1. Referent: Prof. Dr. K.H. Bennemann

2. Referent: Prof. Dr. J. Koutecký

Tag der mündlichen Prüfung: 30. Juni 1977

Digitized by the Internet Archive
in 2026

https://archive.org/details/IA41549616_0053

This work was carried out
under the supervision of

Prof. Dr. K. H. BENNEMANN

at the Institute of Theoretical Physics
of the Freie Universität Berlin
West Germany

I am very much obliged to Prof. Dr. K.H. Bennemann for suggesting the topics covered in this dissertation, and for giving me enlightening instruction and continued guidance, assistance and encouragement througout the course of this work.

Fruitful discussions and valuable comments from Prof. Dr. J. Koutecký, Dr. G.Kerker and Dr. A. ten Bosch are gratefully acknowledged.

This work was partly supported by Consejo Nacional de Ciencia y Tecnología, México.

TABLE OF CONTENTS

		Page
I.	INTRODUCTION	7
II.	A) THEORY FOR d-ELECTRONS NEAR AN ALLOY SURFACE	19
	B) NUMERICAL RESULTS FOR THE DENSITY OF STATES NEAR THE SURFACE OF TRANSITION METAL ALLOYS	28
	C) CHEMISORPTION AT THE SURFACE OF TRANSITION METAL ALLOYS	37
III.	SEGREGATION AT THE SURFACE OF TRANSITION METAL ALLOYS	53
IV.	SELECTIVE CATALYTIC BEHAVIOUR OF THE Cu-Ni ALLOY SURFACE	73
V.	ORDER-DISORDER PHASE TRANSITION AT THE SURFACE OF BINARY ALLOYS	82
VI.	CONCLUSIONS	101

		Page
APPENDIX A.	DETERMINATION OF G_{ii} IN THE PRESENCE OF s-d HYBRIDIZATION	105
APPENDIX B.	COHERENT POTENTIAL APPROXIMATION AND ITS EXTENSION THE BETHE-PEIERLS APPROXIMATION FOR AN ALLOY SURFACE	107
APPENDIX C.	DETERMINATION OF THE INTERNAL ENERGY IN THE BRAGG-WILLIAMS APPROXIMATION AS A FUNCTION OF THE ORDER PARAMETERS	110
APPENDIX D.	ELECTRONIC THEORY FOR THE ORDER-DISORDER TRANSITION AT THE SURFACE OF BINARY ALLOYS	115
REFERENCES		125

I. INTRODUCTION

It has been observed that transition metals exhibit particular interesting surface phenomena. In particular, transition metals play an important role for chemisorption and catalysis, presumably due to the d-electrons[1-4]. Furthermore, experiments have shown [5,6] that transition metal alloys like Cu-Ni alloys exhibit catalytic behaviour with interesting technical applications.

Recently, the behaviour of d-electrons near transition metal surfaces has been studied[7-11] as well as the problem of chemisorption on metals[12-17]. None of these theoretical studies have been extended to alloy surfaces[18]. Since in alloys the electronic parameters can be varied continuously, alloys are particularly interesting for recognizing the important electronic parameters determining surface properties.

In this work we present a theory for the electronic structure at the surface of transition metal alloys as well as for atoms chemisorbed at such surfaces. We apply our theory to calculate the local density of states and to determine the variation of the binding energy of chemisorbed atoms as a function of alloy composition, adatom position and surface environment. We also apply our theory to treat important surface phenomena like segregation and

order-disorder phase transition.

It is important to study atomic segregation to understand the properties of transition metal alloy surfaces. The catalytic activity is mainly determined by the surface composition and it is in general found experimentally that the composition in the surface and in bulk are different[19-21].

As in the case of magnetism, superconductivity, melting, etc. one might expect that the order-disorder phase transition is affected by the surface. One would like to know for example, over which distance away from the surface the order parameter is affected by the surface, how the effect of the surface depends on the geometry of the surface and how atomic segregation affects the order-disorder phase transition.

In the following the experimental situation is described in more detail. Recently, the application of alloys as catalysts has grown considerably, especially in oil-refining processes[22]. Most industrial chemical processes are promoted by catalysts, so that catalysis has been object of extensive scientific investigations. So far the understanding of the fundamental processes involved is not complete. Metal catalysts have long been known and used in chemical industry. The observation that most elements showing measurable catalytic activity are transition

metals of the Group VII and IB lead to correlate the d-electron character of the metalic bond with the catalytic activity. It is not yet well understood how catalytic activity for a given reaction varies from one material to another. For elements and simple compounds an empirical catalog can be established. It is obvious that alloys are particularly interesting. By alloying two metals of different catalytic properties a new catalist can be obtained. Catalysts are no longer selected they are designed.

It is observed that the catalytic activity of alloys vary very rapidly with composition[5,23]. If one of the metals is practically inactive, two effects have to be considered. Alloying changes the strength of the metal-adsorbate bond (chemical effect) and the atomic environment (geometrical effect). An example is the hydrogenolysis (dissociation by the action of hydrogen) of ethane over copper-nickel catalysts

$$H_3C - CH_3 + H_2 \rightarrow 2CH_4$$

Here the catalytic activity decreases strongly as the copper content increases[5]. In contrast to hydrogenolysis, the catalytic activity for reactions where the simple adition or substraction of hydrogen (hydrogenation and dehydrogenation) takes place, remains almost constant over the

whole range of concentrations. This behaviour is shown in Fig. 1.

In order to explain the catalytic behaviour as a function of alloy surface composition, we need some information about the composition of the actual surface exposed to the reacting molecules. There is experimental evidence that generally segregation accurs at the surface of alloys. Using several methods, like work function measurements[19], selective chemisorption[20], Auger spectroscopy[21], etc., it has been well established that the surface and bulk compositions can be appreciably different. In Fig. 2 experimental results on segregation at the surface of Cu-Ni alloys are shown[5]. It is obvious from these results, that it is important to include segregation in order to analyse properly the strength of the chemical bond between absorbed molecules and Ni, for example on Cu-Ni alloys.

In low-energy electron diffraction experiments has been found that in ordered alloys the order-disorder phase transition is affected by the surface[24]. Experimentally the temperature dependence of the order parameter is studied. However, no experimental results on surface order-disorder transitions as well as quenching of the order state at the surface and the effect of segregation in the order-disorder transition are available. Experimental

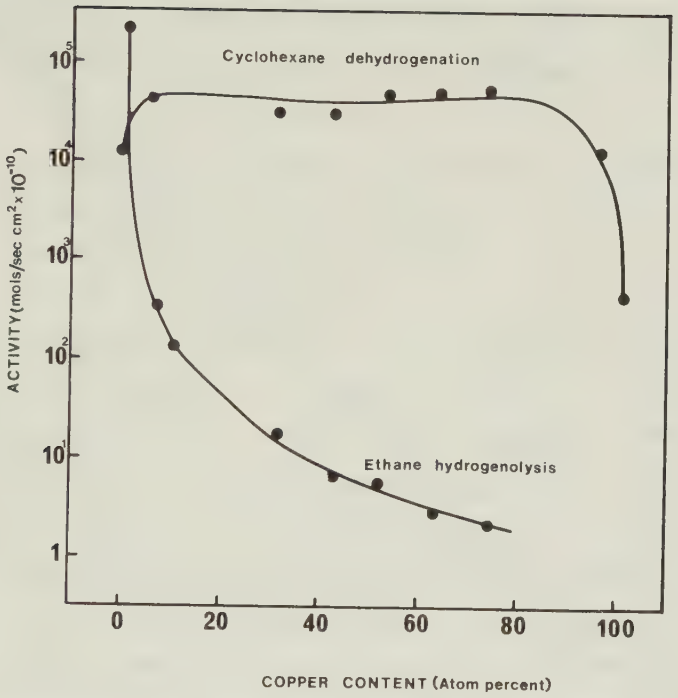

Fig. 1 Specific activities of Cu-Ni alloy catalysts for hydrogenolysis of ethane to methane and dehydrogenation of cyclohexane to benzene at 316^{o}C [5].

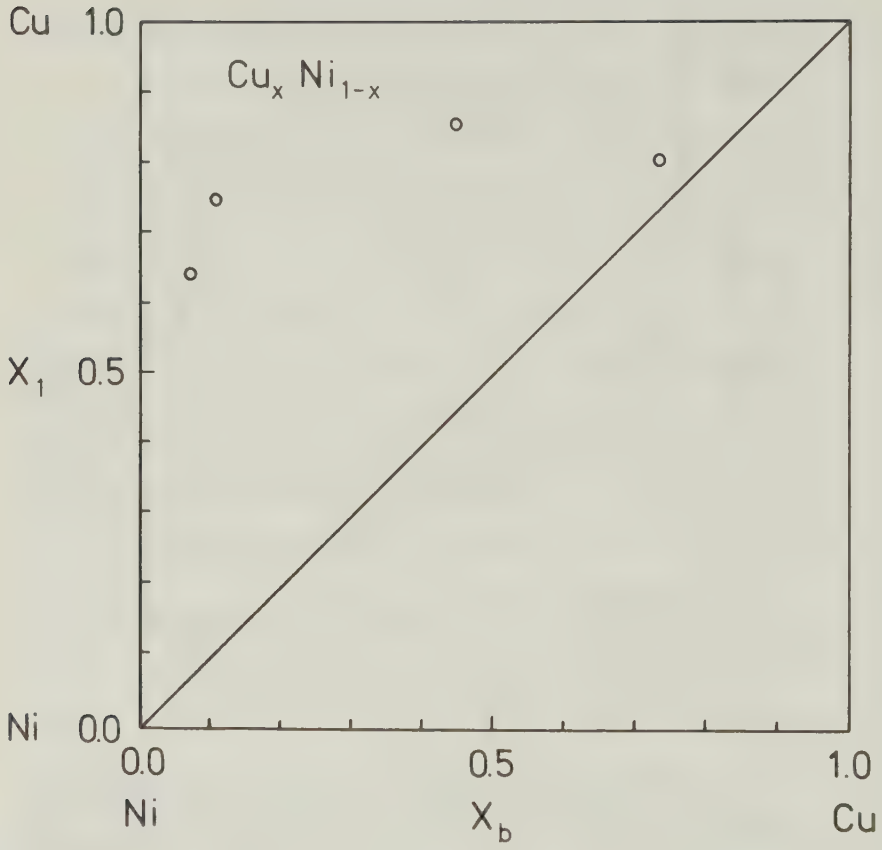

Fig. 2 Experimental results for the segregation in Cu_xNi_{1-x} alloys at room temperature[5]. x_1 and x_b refer to the Cu-concentration at the surface and in bulk respectively.

results are shown in Fig. 3. Furthermore to study environment effects it is interesting to study chemisorption near order-disorder transitions since the probabilities to find a pair, triplet, etc., of active sites, needed for some reactions to occur, are functions of the surface long range order parameter. The effect of long range order on the surface composition is also of interest.

All these experimental facts have lead to an intensive theoretical study of the behaviour of d-electrons near transition metal surfaces. In the frame of the tight-binding model, well suited to treat d-electrons, several theories for the electronic structure at the surface of pure metals have been presented. The continued fraction method[8,9] and the moment method[10,11] are examples. Using these methods, the dependence of the electronic structure at one atomic site on the local atomic environment can be studied. Therefore, these local theories can be applied to the electronic structure at the surface in the presence or absence of absorbed atoms. Within these formalisms various surface properties, like for example the surface tension[25], can be explained. Chemisorption of atoms and molecules at the surface of pure metals has also been developed[12-17]. However, none of these theories have been extended to treat alloy surfaces.

Theories for the electronic structure of bulk dis-

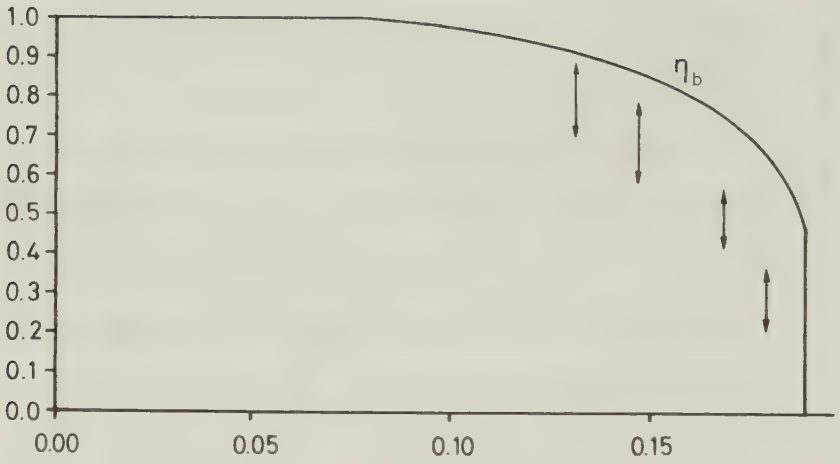

Fig. 3 Measured long-range order parameters as a function of temperature for the (100) surface of Cu_3Au. The order parameter for the surface is shown by the arrows. η_b refers to the order-parameter bulk.

ordered binary alloys have been developed in the last few years[26-33]. These theories have been generally discussed using the tight-binding approximation and the multiple-scattering theory[34]. The multiple scattering is treated self-consistently with the mean field approximation, whereby the alloy is descomposed into a sum of individual atomic scatterers[35-38]. The scattering of the electrons by the atomic disorder leads to renormalize the electronic energies which is for the bulk space independent. However, in the precence of the surface, the electronic self-energies resulting from the scattering by the atomic disorder becomes space dependent and vary for the first few atomic layers parallel close to the surface. We show in this work how the bulk theory has to be modified to take this into account. Due to the complexity of the theory we use only the most simple version of our surface theory. We assume that only the surface layers have a self-energy different from the whole crystal[39,40]. This model is illustrated in Fig. 4.

It is the aim of this work to present an electronic theory for the surface of transition metal alloys as well as for atoms chemisorbed at such surfaces. This theory is developed by using the tight-binding Hamiltonian and determining the electronic Green's function by using the continued fraction method[8,9]. This method is the most appropia-

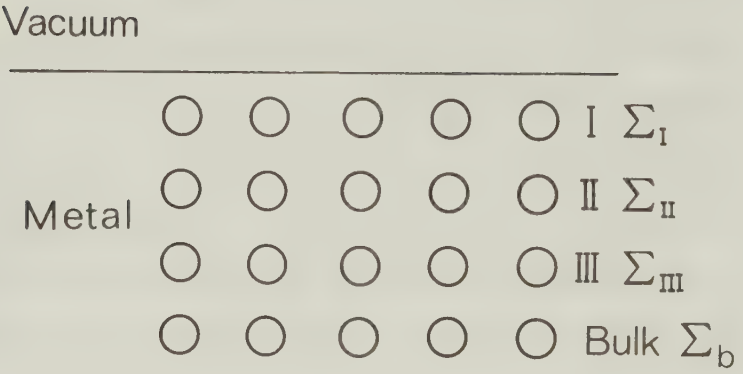

Fig. 4 Illustration of the surface model used in this work. Σ_I, Σ_{II}, Σ_{III} and Σ_b are the are the average electron energies at the firs, second, third and bulk layers respectively.

te to treat surface properties depending on the local atomic environment and to analyse the experimental results refered earlier. Although the theory developed is simpler than the coherent potential approximation it is interesting to note that the results for the electronic density of states are nearly the same for both approaches.

In Chapter IIA) we present the theory for the d-electrons at the surface of transition metal alloys[39]. The numerical results for the local density of states are presented in Chapter IIB). In Chapter IIC) we extend our theory to treat chemisorption of atoms at alloy surfaces. We determine the dependence of the binding energy on alloy composition, adatom position and local atomic environment[41].

In Chapter III we apply our theory to surface segregation[42]. Here we study for different concentrations the dependence of segregation on the electronic parameters and illustrate the importance of segregation segregation for analysing the composition dependence of the binding energy of atoms chemisorbed at the surface.

We apply in Chapter IV our results on the binding energy of atoms chemisorbed at the surface of Cu-Ni alloys and the results for segregation at such surfaces to explain the selectivity[5,22,23] of Cu-Ni alloy catalysts.

In Chapter V we study the order-disorder phase tran-

sitions at the surface of binary alloys. We show the importance of segregation in the order-disorder phenomena[43]. In Chapter V the results are summarized and other further interesting applications are discussed.

In appendix A we determine the local electronic Green function G_{ii} in the precense of s-d hybridization. We present in appendix B an extension to the coherent potential approximation (Bethe-Peierls approximation) for an alloy surface. In appendix C we give details of the determination of the internal energy using the Bragg-Williams approximation and outline in appendix D a microscopic theory for order-disorder phenomena at the surface.

II.A) THEORY FOR d-ELECTRONS NEAR AN ALLOY SURFACE

The electrons in a binary alloy A_xB_{1-x} with substitutional disorder are described by the tight-binding Hamiltonian

$$H = \sum_{i=A,B} \varepsilon_i c_i^\dagger c_i + \sum_{i \neq j} t_{ij} c_i^\dagger c_j, \qquad \text{II.1}$$

where the electronic energy levels

$$\varepsilon_i = \varepsilon_i^0 + U_d^i n_i + U_{ds}^i n_i^s, \qquad \text{II.2}$$

can take the values ε_A or ε_B depending on whether the site i is occupied by an A- or B-atom. Here, U_d^i denotes the inter- atomic Coulomb interaction on site i with n_i d-electrons and U_{ds}^i denotes the Coulomb interaction between d- and s-electrons on site i. The energies ε_i^0 are supposed to take into account s-d hybridization. The hopping integrals t_{ij} which describe electronic transitions between states centered on atomic sites i and j are assumed concentration independent. $c_i^\dagger$ and c_i are the usual creation and annihilation operators for d-electrons on site i.

The local electronic Green's function G_{ii} describing d-electrons on the atom i is given by

$$G_{ii}(E) = (E - \varepsilon_i - \Delta_i)^{-1} \qquad \text{II.3}$$

where the electron self-energy Δ_i resulting from the hopping of the electrons between the atoms is given by

$$\Delta_i = \sum_{j\neq i} \frac{t_{ij}t_{ji}}{E-\varepsilon_j-\Delta_j^i} + \sum_{\substack{j\neq i \\ \ell\neq i,j}} \frac{t_{ij}t_{j\ell}t_{\ell i}}{(E-\varepsilon_j-\Delta_j^i)(E-\varepsilon_\ell-\Delta_\ell^{ij})} + \ldots \qquad \text{II.4}$$

with

$$\Delta_j^i = \sum_{\ell\neq i,j} \frac{t_{j\ell}t_{\ell j}}{E-\varepsilon_\ell-\Delta_\ell^{ij}} + \sum_{\substack{\ell\neq i,j \\ m\neq i,j,\ell}} \frac{t_{j\ell}t_{\ell m}t_{mj}}{(E-\varepsilon_\ell-\Delta_\ell^{ij})(E-\varepsilon_m-\Delta_m^{ij\ell})} + \ldots \qquad \text{II.5}$$

which results from all electron hopping processes starting and ending at the site j and avoiding the sites i and j in-between. The self enrgies Δ_ℓ^{ij} and $\Delta_m^{ij\ell}$ result from d-electron hopping processes avoiding sites i,j,ℓ,m and are given by expresions which are similar to the one for Δ_j^i.

The determination of $G_{ii}(E)$ in bulk within the coherent potential approximation (CPA), is obtained by replacing the electron energies ε_i by an average energy Σ in equations II.4 and II.5. It is interesting to note that we get escentially the same results for the bulk electron density of states as obtained by Velický et al.[36] using CPA if we keep only the t^2-terms in the expansion for Δ_i and Δ_j^i and use the approximation $\Delta_\ell^{ij} = \Delta_\ell^j$.

Within these approximations we obtain for the bulk the equation

$$\Delta_b^b = (Z-1)\,t^2\left(\frac{x}{E-\epsilon_A-\Delta_b^b}+\frac{1-x}{E-\epsilon_B-\Delta_b^b}\right), \qquad \text{II.6}$$

which can be rewriten as a third order equation[46] for Δ_b^b

$$(\Delta_b^b)^3-2E(\Delta_b^b)^2+\left[E^2+\epsilon_A\epsilon_B+(Z-1)t^2\right]\Delta_b^b - (Z-1)\,t^2\left[E-\epsilon_B x-\epsilon_A(1-x)\right]=0 \qquad \text{II.7}$$

Here, Z denotes the number of nearest neighbors, $t_{ij}=t$ for nearest neighbor atoms and $\Delta_j^i=\Delta_b^b$ means that the sites i and j are bulk sites.

The appropiate solution of equation II.7 gives the bulk average electron Green's function

$$G_b(E) = xG_A + (1-x)G_B \qquad \text{II.8}$$

The above theory is now applied to d-electrons at the surface of transition metal alloys. Near the surface the Green's function $G_{ii}(E)$ depends not only in the type i of atom but also in the perpendicular distance from the surface. Therefore, we use for the Green's function the notation $G_{L,i}$ which describes d-electrons at atoms of sort i in the L-th atomic layer parallel to the surface. The

average electron Green's function in the first atomic layer is

$$G_I(E) = xG_{I,A} + (1-x)G_{I,B} \qquad \text{II.9}$$

where

$$G_{I,i}(E) = (E - \varepsilon_{I,i} - \Delta_I)^{-1} \qquad \text{II.10}$$

Here, $\varepsilon_{I,i}$ denotes ε_i for atomic sites in the first layer. Similarly, the Green's functions G_{II}, $G_{II,i}$, G_{III}, $G_{III,i}$, etc. refer to d-elctrons in the second, third, etc. layer away from the surface. For simplicity we assume now that the effects due to the surface are significant only within the first three surface layers as it is illustrated in Fig. 4. Therefore, we use for the atomic sites beyond the first three atomic surface layers the bulk Green's function given by equation II.10.

Using equation II.4 we obtain for the self-energies Δ_I, Δ_{II} and Δ_{III} the expresions

$$\Delta_I = Z_0 t^2 \left(\frac{X_I}{E - \epsilon_{I,A} - \Delta_I^I} + \frac{1 - X_I}{E - \epsilon_{I,B} - \Delta_I^I} \right)$$

$$+ Z_1 t^2 \left(\frac{X_{II}}{E - \epsilon_{II,A} - \Delta_{II}^I} + \frac{1 - X_{II}}{E - \epsilon_{II,B} - \Delta_{II}^I} \right),$$

$$\Delta_{II} = Z_0 t^2 \left(\frac{x_{II}}{E - \epsilon_{II,A} - \Delta_{II}^{II}} + \frac{1 - x_{II}}{E - \epsilon_{II,B} - \Delta_{II}^{II}} \right) + Z_1 t^2 \left(\frac{x_I}{E - \epsilon_{I,A} - \Delta_I^{II}} + \frac{1 - x_I}{E - \epsilon_{I,B} - \Delta_I^{II}} \right)$$

$$+ Z_1 t^2 \left(\frac{x_{III}}{E - \epsilon_{III,A} - \Delta_b^{II}} + \frac{1 - x_{III}}{E - \epsilon_{III,B} - \Delta_b^{II}} \right) ,$$

$$\Delta_{III} = Z_0 t^2 \left(\frac{x_{III}}{E - \epsilon_{III,A} - \Delta_b^b} + \frac{1 - x_{III}}{E - \epsilon_{III,B} - \Delta_b^b} \right) + Z_1 t^2 \left(\frac{x_{II}}{E - \epsilon_{II,A} - \Delta_{II}^b} + \frac{1 - x_{II}}{E - \epsilon_{II,B} - \Delta_{II}^b} \right)$$

$$+ Z_1 t^2 \left(\frac{x_b}{E - \epsilon_A - \Delta_b^b} + \frac{1 - x_b}{E - \epsilon_B - \Delta_b^b} \right) .$$

In deriving these equations we have performed the summation over nearest neighbors neglecting terms of higher order than t^2 in equation II.4. Here, Z_0 denotes the number of nearest neighbor atoms within the same layer and Z_1 the number of nearest neighbor atoms within one of the nearest neighbor layers. The concentrations of A atoms in the first, second and third layers are x_I, x_{II} and x_{III} respectively. The electronic energies $\epsilon_{I,A}$, $\epsilon_{I,B}$, $\epsilon_{II,A}$, etc., denote the energy ϵ_i for atoms A and B in the first surface layer I, second surface layer II, etc. Notice that $\Delta_j^i = \Delta_I^I$ if i and j refer to atomic sites in the first surface layer. Similarly $\Delta_j^i = \Delta_{II}^I$ if i refers to a site in the first atomic layer and j to the second surface layer.

In the derivation of equations II.11-II.13 we have used the approximation $t_{ij} = t$ for all layers. Relaxation

effects in the surface can be incorporated to the theory using appropiate values for $t_{I,I}, t_{I,II}$, etc. different from the value of the hopping integral in bulk.

For determining Δ^i_j we use the approximation $\Delta^{ij}_\ell = \Delta^j_\ell$ which is exact for a Bethe lattice[46,47]. Then we find

$$\Delta^{I}_{I} = (Z_0 - 1)t^2\left(\frac{X_I}{E-\epsilon_{I,A}-\Delta^{I}_{I}} + \frac{1-X_I}{E-\epsilon_{I,A}-\Delta^{I}_{I}}\right) + Z_1 t^2\left(\frac{X_{II}}{E-\epsilon_{II,A}-\Delta^{II}_{II}} + \frac{1-X_{II}}{E-\epsilon_{II,B}-\Delta^{II}_{II}}\right)$$

$$\Delta^{I}_{II} = Z_0 t^2\left(\frac{X_{II}}{E-\epsilon_{II,A}-\Delta^{II}_{II}} + \frac{1-X_{II}}{E-\epsilon_{II,B}-\Delta^{II}_{II}}\right) + (Z_1-1)t^2\left(\frac{X_I}{E-\epsilon_{I,A}-\Delta^{II}_{I}} + \frac{1-X_I}{E-\epsilon_{I,B}-\Delta^{II}_{I}}\right)$$

$$+ Z_1 t^2\left(\frac{X_{III}}{E-\epsilon_{III,A}-\Delta^{II}_{b}} + \frac{1-X_{III}}{E-\epsilon_{III,B}-\Delta^{II}_{b}}\right)$$

$$\Delta^{II}_{II} = (Z_0 - 1)t^2\left(\frac{X_{II}}{E-\epsilon_{II,A}-\Delta^{II}_{II}} + \frac{1-X_{II}}{E-\epsilon_{II,B}-\Delta^{II}_{II}}\right) + Z_1 t^2\left(\frac{X_I}{E-\epsilon_{I,A}-\Delta^{II}_{I}} + \frac{1-X_I}{E-\epsilon_{I,B}-\Delta^{II}_{I}}\right)$$

$$+ Z_1 t^2\left(\frac{X_{III}}{E-\epsilon_{III,A}-\Delta^{II}_{b}} + \frac{1-X_{III}}{E-\epsilon_{III,B}-\Delta^{II}_{b}}\right)$$

$$\Delta_I^{II} = Z_0 t^2 \left(\frac{X_I}{E - \epsilon_{I,A} - \Delta_I^I} + \frac{1 - X_I}{E - \epsilon_{I,B} - \Delta_I^I} \right) + (Z_1 - 1) t^2 \left(\frac{X_{II}}{E - \epsilon_{II,A} \Delta_{II}^I} + \frac{1 - X_{II}}{E - \epsilon_{II,A} \Delta_{II}^I} \right)$$

$$\Delta_b^{II} = Z_0 t^2 \left(\frac{X_{III}}{E - \epsilon_{III,A} \Delta_b^b} + \frac{1 - X_{III}}{E - \epsilon_{III,B} - \Delta_b^b} \right) + (Z_1 - 1) t^2 \left(\frac{X_{II}}{E - \epsilon_{II,A} \Delta_{II}^b} + \frac{1 - X_{II}}{E - \epsilon_{II,B} \Delta_{II}^b} \right)$$

$$+ Z_1 t^2 \left(\frac{X}{E - \epsilon_A - \Delta_b^b} + \frac{1 - X}{E - \epsilon_B - \Delta_b^b} \right)$$

and finally

$$\Delta_{II}^b = Z_0 t^2 \left(\frac{X_{II}}{E - \epsilon_{II,A} \Delta_{II}^{II}} + \frac{1 - X_{II}}{E - \epsilon_{II,B} \Delta_{II}^{II}} \right) + Z_1 t^2 \left(\frac{X_I}{E - \epsilon_{I,A} \Delta_I^{II}} + \frac{1 - X_I}{E - \epsilon_{I,B} \Delta_I^{II}} \right)$$

$$+ (Z_1 - 1) t^2 \left(\frac{X_{III}}{E - \epsilon_{III,A} - \Delta_b^{II}} + \frac{1 - X_{III}}{E - \epsilon_{III,B} \Delta_b^{II}} \right)$$

We get a set of six coupled equations with Δ_I^I, Δ_{II}^I, Δ_I^{II} Δ_{II}^{II}, Δ_b^{II} and Δ_{II}^b as unknowns in terms of t, Z_0, Z_1, $\epsilon_{I,i}$, $\epsilon_{II,i}$, $\epsilon_{III,i}$ the bulk energy levels ϵ_i and Δ_b^b. Thus, the electronic Green's functions $G_{I,i}$, $G_{II,i}$ and $G_{III,i}$ are determined by solving these six coupled equations.

The electronic density of states for an atom of type

i in the j-th layer is determined from the electronic Green's function by the formula

$$N_{j,i}(E) = -\frac{1}{\pi} \operatorname{Im} G_{j,i}(E). \qquad \text{II.19}$$

In determining the d-electron Green's functions $G_{j,i}$ we have assumed that the surface affects only the three atomic layers at the surface. This assumption seems reasonable in view of previous tight-binding type calculations at pure metal surfaces[9] and it simplifies considerably the numerical calculations. However, notice that the theory for alloy surfaces can be easily extended to the case where we allow also the fourth, fifth, etc. surface layer to be affected by the surface. Furthermore, in the determination of $G_{j,i}$ we have neglected the contributions to Δ_i and Δ_j^i which are of higher order than t^2. It is known from calculations for the bulk, that these approximations affect essentially only the fine structure in $N_{j,i}(E)$, but should in general not be of essential significance for an exploratory model calculation and for determining the concentration dependence of $N_{j,i}(E)$, the binding energy of chemisorbed atoms, electron charge transfer, etc.

For determining Δ_j^i we have used the approximation $\Delta_\ell^{ij} = \Delta_\ell^j$. To get a feeling for this approximation one

should remember that Δ_{ℓ}^{ij} is obtained from Δ_{ℓ}^{j} if one avoids in determining Δ_{ℓ}^{j} hopping processes which involve the atomic site i. Thus, the approximation on Δ_{ℓ}^{ij} should become better at the surface since the number of neglected paths is smaller.

II.B) NUMERICAL RESULTS FOR THE DENSITY OF STATES NEAR THE SURFACE OF TRANSITION METAL ALLOYS

In this section we present the average and local densities of states in the first three layers at the surface (100) of a fcc lattice. From the agreement between experiment and theory (CPA, etc.) we conclude that the approximations used in our alloy surface theory are valid for Cu-Ni alloys. Therefore, in our calculations we use parameters corresponding to Cu-Ni alloys[48]. In Cu-Ni alloys one can neglect electronic charge transfer between the Cu and Ni atoms. This is plausible since the Fermi energy of Cu and Ni are almost the same.

In the following we express the energy in units of 0.1227 Ry which is half of the Cu d-band. We take for $\delta = \varepsilon_{Ni} - \varepsilon_{Cu}$ the value 1.02 and use $t = 0.206$ in accordance to prior bulk calculations[48].

The Fermi energy E_F is calculated selfconsistently by using[49]

$$\int_{-\infty}^{\varepsilon_F} N_{AV}(E)dE = xN_{Cu} + (1 - x)N_{Ni} \qquad \text{II.20}$$

where $N_{AV}(E)$ is the average bulk density of states, $N_{Cu} = 10$ and $N_{Ni} = 9.45$ electrons.

The approximations used are essentially the same used in CPA calculations in bulk Cu-Ni alloys and should have the same validity. These approximations should apply as well to a number of other transition metal alloys like Rh-Ni, Ag.Pd, etc. for example.

In Fig. 5 we show results for the average local d-electron density of states for concentrations $x = 0.2$ and $x = 0.4$ in the first three surface layers and in a bulk layer. In Fig. 6 we show the local density of states on Cu, Ni and average sites for the same concentrations in the first surface layer. All these results are obtained by using $\delta_i = \varepsilon_{i,A} - \varepsilon_{i,B} = \delta_{bulk}$, $i = 1,2,3$. Notice that this assumption implies electron charge transfer between the atomic layers at the surface. The average number of electrons per site in the i-th layer is namely then different from the corresponding number at a bulk site. This is found from $n_i = \int N_i(E)dE$.

Consequently, allowing no d-electron charge transfer between the surface layers ($n_{d,i} = n_{d,bulk}$) implies layer dependent shifts in the difference $\delta_i = \varepsilon_{i,A} - \varepsilon_{i,B}$ of the energy levels. Here, δ_i refers to the i-th atomic surface layer. These shifts are then calculated by using

$$\int_{-\infty}^{E_F} dE\{N_i(E,\delta_I,\delta_{II},\delta_{III}) - N_{bulk}(E)\} \quad i=I,II,III \qquad II.21$$

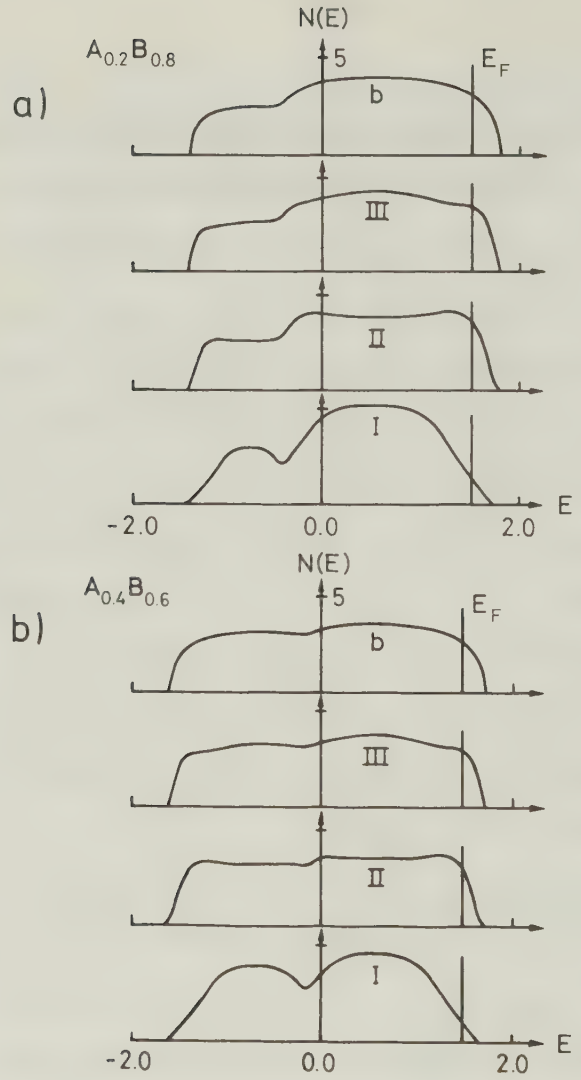

Fig. 5 Average density of states $N_i(E)$ of the first three surface layers (i=I,II,III) and a bulk layer b of an alloy A_xB_{1-x} corresponding to Cu_xNi_{1-x}:a) x=0.2, b) x=0.4. The zero of energy is such that $\varepsilon_{Cu}=-.51=-\delta/2$ and $\varepsilon_{Ni}=\delta/2$.

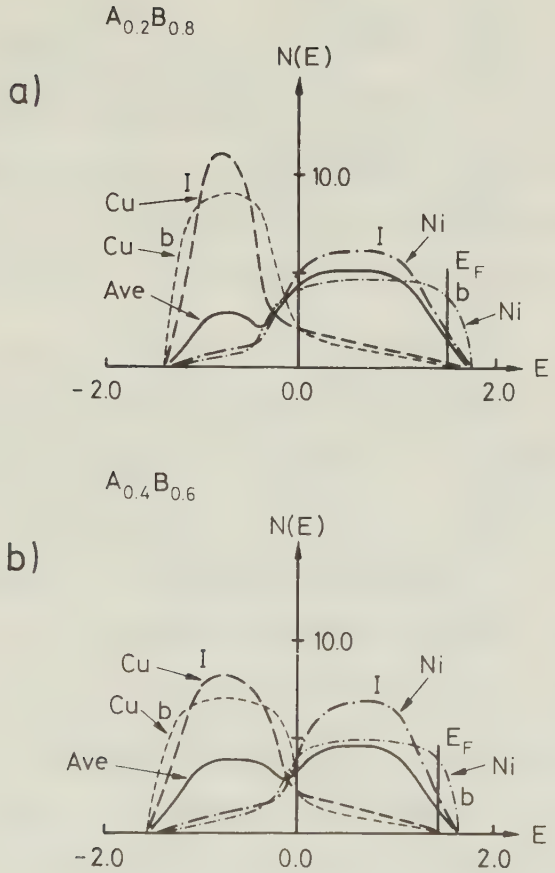

Fig. 6 Local density of states per atom $N_i(E)$ for different concentrations in an alloy corresponding to Cu_xNi_{1-x}. The labels Cu, Ni and Ave refer to a Cu site, a Ni site and an average site, respectively. The curves labeled I and b refer to the surface layer and the bulk, respectively.

for the first three layers.

In Figs. 7 and 8 we show how the local density of states shown in Fig. 5 and 6 are modified for the case where no d-electron charge transfer is allowed between the surface layers. In Fig. 9 we show how $\delta_i = \varepsilon_{i,A} - \varepsilon_{i,B}$, i =I,II changes with concentration. δ_{III} is almost equal to δ_{bulk}.

In order to calculate the change Δn_i in n_i due to electronic charge transfer we have to determine ε_i selfconsistently using $\varepsilon_i = \varepsilon_i^o + Un_i$. This does not change the theory presented but only complicates the numerical analysis. Notice that d-electron conservation implies $\Delta n_i = 0$. If s- and d-electrons are treated together then one obtains $\Delta n_i^d + \Delta n_i^s = 0$ where Δn_i^s is the change in the number of s-electrons within the Wigner-Seitz cell of the i-th atom due to s → d and d → d charge transfer.[50]

From the results, one sees that mainly only $N_i(E)$ of the first two surface layers is changed with respect to the bulk. As expected, one observes that due to the surface N(E) tends to narrow. The surface has a more dramatic effect on $N_{Ni}(E_F)$ than on $N_{Cu}(E)$. Also as shown in Fig. 5 (which shows results for $\delta_i = \delta_{bulk}$, i = I,II,III, implying d-electron charge transfer between the layers at the surface) and Fig. 7 (which shows results for $\delta_i \neq \delta_{bulk}$

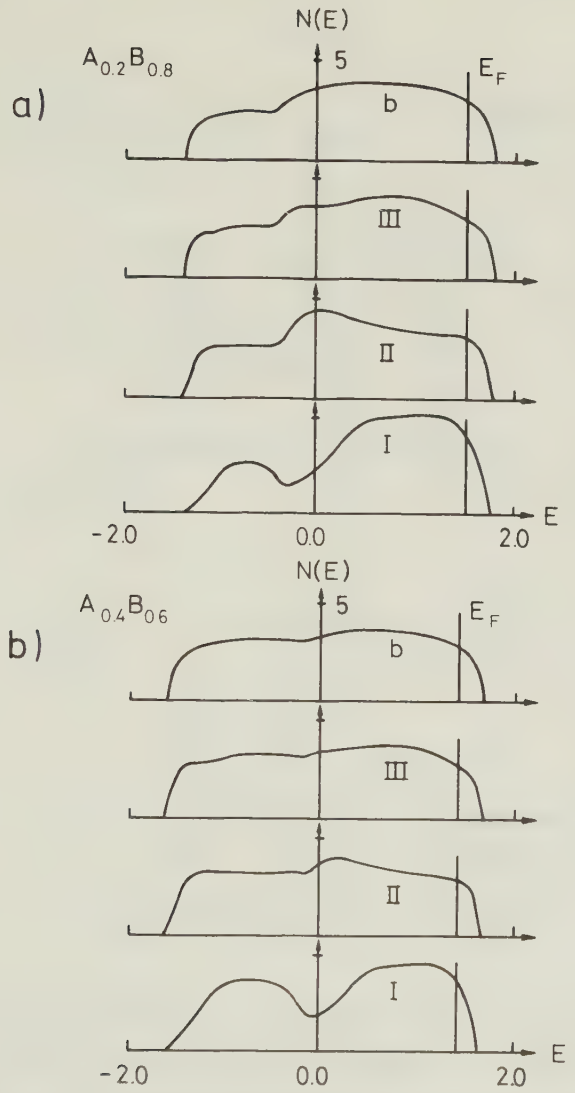

Fig. 7 Average density of states $N_i(E)$, for x=0.2 and x=0.4, of the first three surface layers (i=I,II,III) and a bulk layer b of an Cu_xNi_{1-x} alloy, assuming no electron charge transfer between the surface layers.

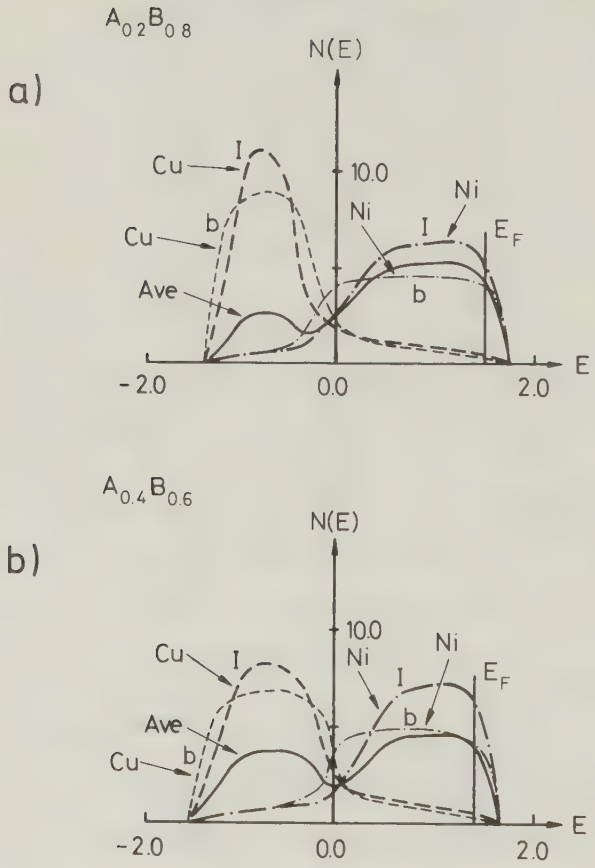

Fig. 8 Local density of states of the surface layer $N_{I,i}(E)$, and for the bulk $N_b(E)$ on a Cu site, on a Ni site, and on an average site. No electron charge transfer between the surface layers is allowed.

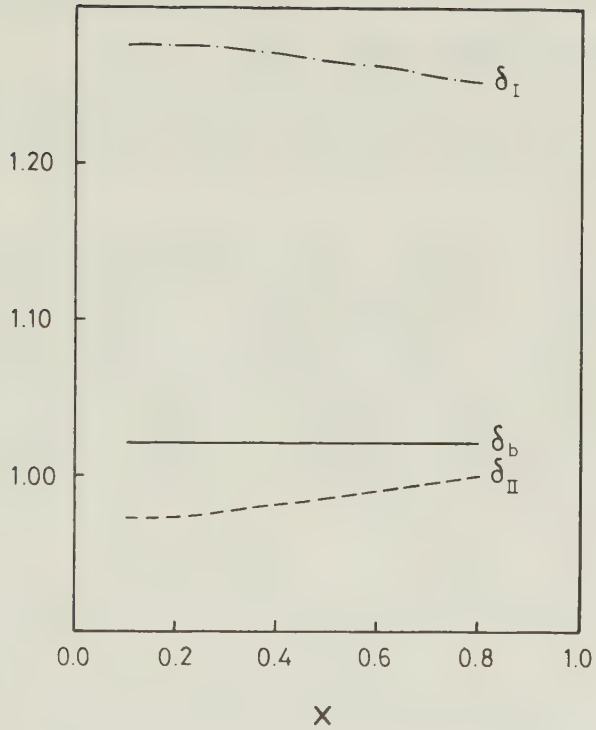

Fig. 9 Concentration dependence of $\delta_{I=\varepsilon_{I,Ni}-\varepsilon_{I,Cu}}$ and $\delta_{II=\varepsilon_{II,Ni}-\varepsilon_{II,Cu}}$ in energy units of half of the Cu d-band width. We take for the bulk $\delta_b=1.02$.

such that no d-electron charge transfer occurs) electron charge transfer affects mainly only $N_{Ni}(E)$. This will also be the case if the electron charge transfer results from adatoms or s-d transitions.

II.C) CHEMISORPTION AT THE SURFACE OF TRANSITION METAL ALLOYS

To avoid the numerical complications due to electron charge transfer and Coulomb interactions we restrict ourselves to adatoms of the same kind as those of the substrate.

We study how the local density of states on the adatom changes with (a) the alloy composition of the substrate, (b) the local atomic environment of the substrate around the adatom and (c) for different adatom positions.

We calculate the local density of states on the adatom as follows. The Green's function for the adatom is given by

$$G_a(E) = (E - \varepsilon_a - \Delta_a)^{-1} \qquad \text{II.22}$$

where Δ_a is calculated by using the expansion II.4

$$\Delta_a = \sum_{i \neq a} \frac{t'^2}{(E-\varepsilon_i-\Delta_i)} + \sum_{\substack{i \neq a \\ j \neq i,a}} \frac{t'^2 t}{(E-\varepsilon_i-\Delta_i)(E-\varepsilon_j-\Delta_j)} \qquad \text{II.23}$$

Here ε_a is the adatom electronic energy and t' is the hopping integral between the adatom and its nearest neighbor atoms. Δ_i is the first layer renormalization energy

given by equation II.11. To get more detailed information on the shape of the local density of states at the adatom we have included t^3-terms in the expansion II.23 for the local self-energy.

In Fig.10 we show the various adatom positions (A), (B), (C) and the local adatom-substrate configurations (C1), (C2), (C3) and (C4) which we have studied.

In Figs. 11 and 12 results are presented for the local density of states of the adatom when it is in the positions (A), (B) and (C). We use $\epsilon_a = \epsilon_{Ni}$, $t' = t$ and put $x = 0.2$ and $x = 0.4$. In this case the nearest neighbor atoms are taken as average atoms and Δ_a for the (B) position, for example, is given by

$$\Delta_a = Z_a t'^2 \left(\frac{x_I}{E - \epsilon_{I,A} - \Delta_I} + \frac{1 - x_I}{E - \epsilon_{I,B} - \Delta_I} \right)$$

$$+ Z_a t'^2 t \left(\frac{x_I^2}{(E - \epsilon_{I,A} - \Delta_I)(E - \epsilon_{I,A} - \Delta_I^I)} + \frac{x_I(1-x_I)}{(E - \epsilon_{I,A} - \Delta_I)(E - \epsilon_{I,B} - \Delta_I^I)} \right.$$

$$\left. + \frac{x_I(1-x_I)}{(E - \epsilon_{I,B} - \Delta_I)(E - \epsilon_{I,A} - \Delta_I^I)} + \frac{(1-x_I)^2}{(E - \epsilon_{I,B} - \Delta_I)(E - \epsilon_{I,B} - \Delta_I^I)} \right)$$

II.24

Here, Z_a is the number of nearest neighbor atoms of the adatom. In the top position (A) only the first term in equation II.24 is present. For the adatom central position

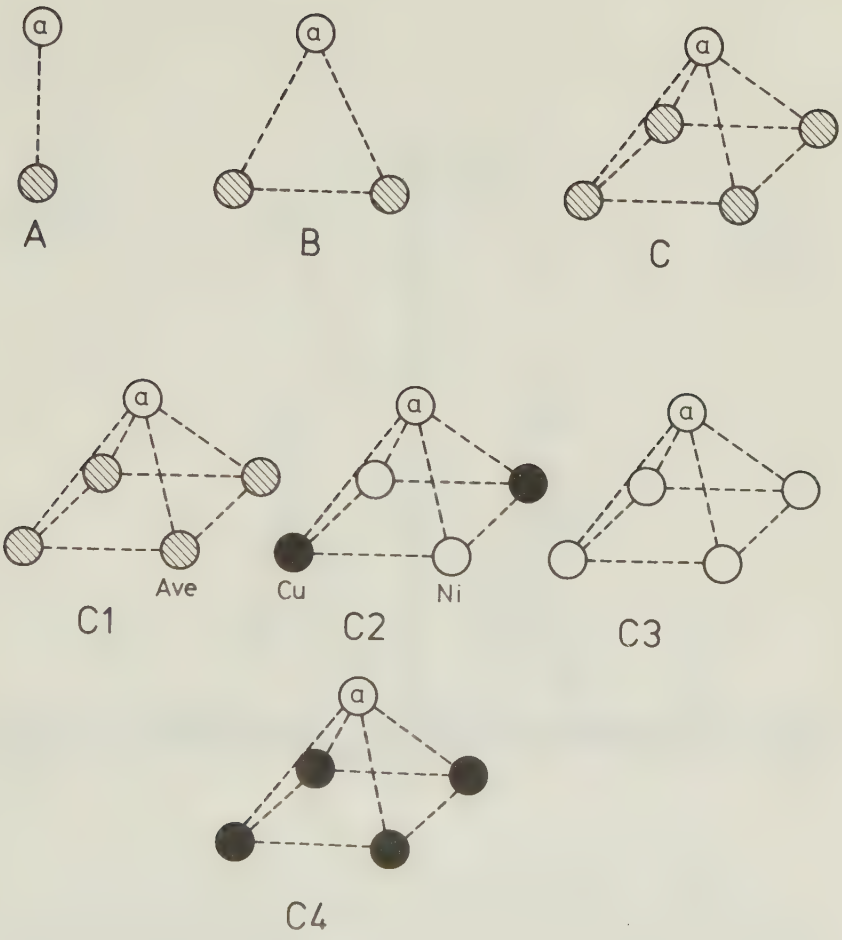

Fig. 10 Different adatom (a) positions A,B and C on a (100)-fcc lattice surface are shown. Also the different adatom-substrate configurations C1, C2, C3 and C4 are shown. The black circles refer to Cu atoms, the open circles to Ni atoms and the dashed circles to average atoms, respectively.

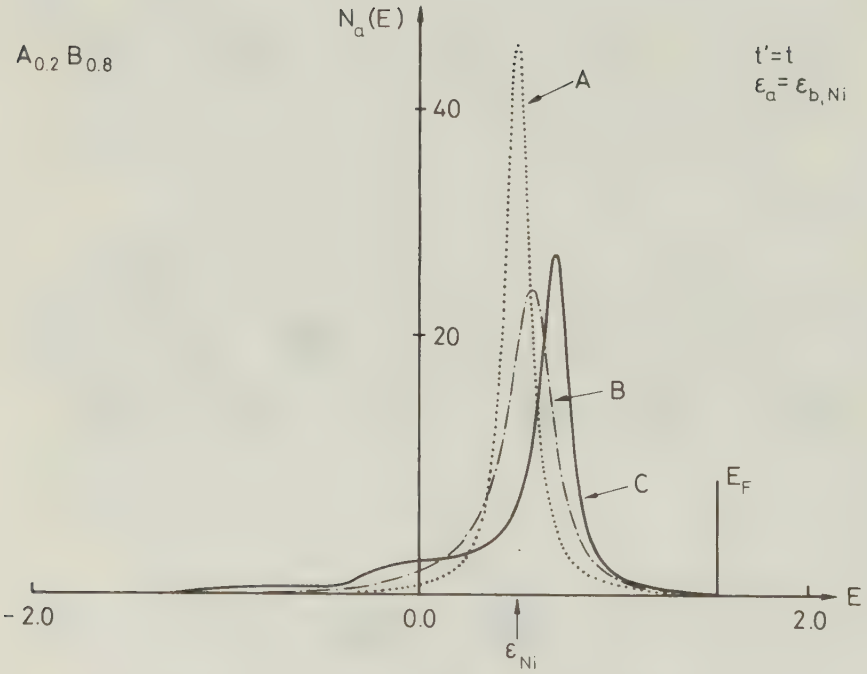

Fig. 11 Local density of states $N_a(E)$ on the adatom for its positions A, B and C for the alloy concentration x=0.2. We put $\varepsilon_a = \varepsilon_{Ni,b}$, $t' = t$, $\delta_i = \delta_b$.

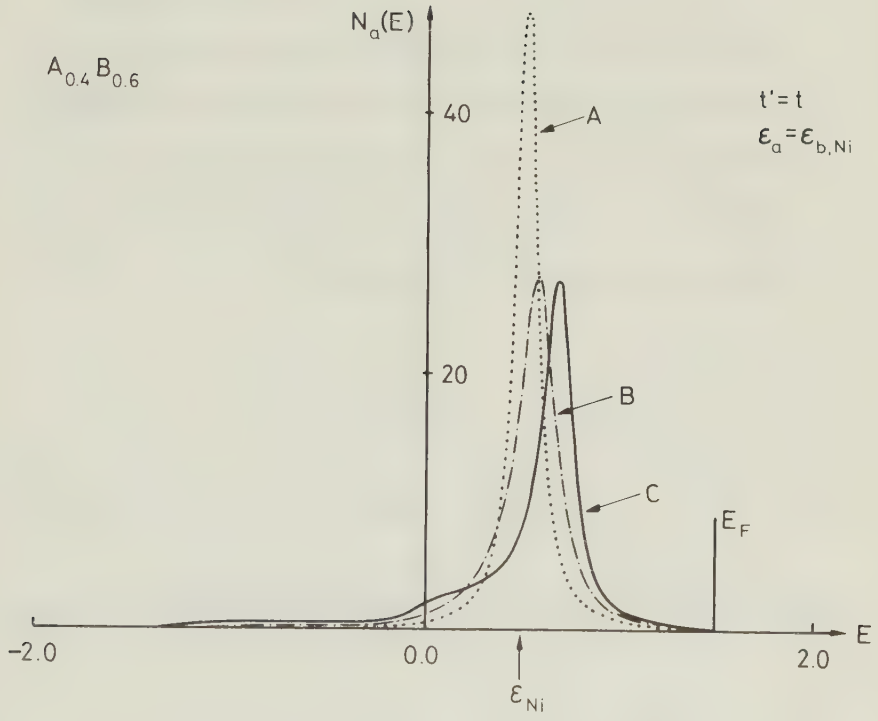

Fig. 12 Local density of states $N_a(E)$ on the adatom for its positions A,B and C. We use $\varepsilon_a=\varepsilon_{Ni,b}$, $t'=t$, $\delta_i=\delta_b$ and the alloy concentration $x=0.4$.

(C) also paths involving four steps are important and have to be considered.

In Figs. 13 and 14 we show results for the adatom local density of states for the substrate configurations (C1), (C2), (C3) and (C4). Here we have used the same parameters as in Figs. 11 and 12 and we have taken exactly into account the environment for configurations (C2), (C3) and (C4). The renormalization energy Δ_a for the (C2) configuration, for example, is given by

$$\Delta_a = 2t'^2\left(\frac{1}{E-\epsilon_{I,A}-\Delta_I} + \frac{1}{E-\epsilon_{I,B}-\Delta_I}\right)$$
$$+ 4t'^2t\left(\frac{1}{(E-\epsilon_{I,A}-\Delta_I)(E-\epsilon_{I,\bar{B}}-\Delta_I^{\bar{I}})} + \frac{1}{(E-\epsilon_{I,B}-\Delta_I)(E-\epsilon_{I,\bar{A}}-\Delta_I^{\bar{I}})}\right)$$
$$+ 4t'^2t^2\left(\frac{1}{(E-\epsilon_{I,A}-\Delta_I)(E-\epsilon_{I,\bar{B}}-\Delta_I^{\bar{I}})(E-\epsilon_{I,\bar{A}}-\Delta_I^{\bar{I}})}\right.$$
$$\left. + \frac{1}{(E-\epsilon_{I,B}-\Delta_I)(E-\epsilon_{I,\bar{A}}-\Delta_I^{\bar{I}})(E-\epsilon_{I,\bar{B}}-\Delta_I^{\bar{I}})}\right). \qquad \text{II.25}$$

In equation II.25 we have taken the same hopping integral t' between the Ni-adatom and the Cu- and Ni-atoms of the substrate. However, the correct values for $t_{a,Cu}$ and

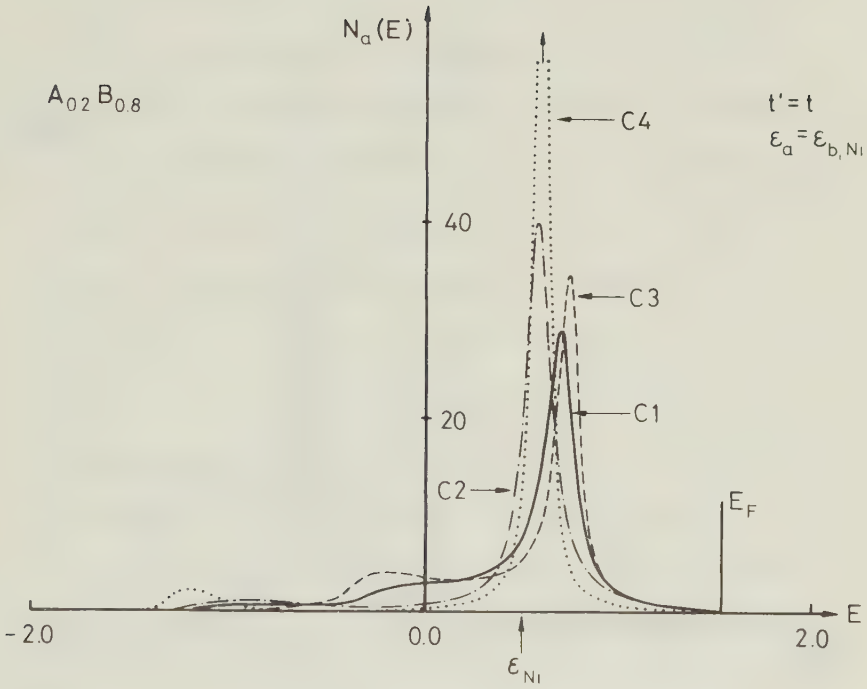

Fig. 13 Local density of states $N_a(E)$ on the adatom for the different substrate configurations C1, C2, C3 and C4. We use $\varepsilon_a=\varepsilon_{Ni,b}$, $t'=t$, $\delta_i=\delta_b$ and the alloy concentration $x=0.2$.

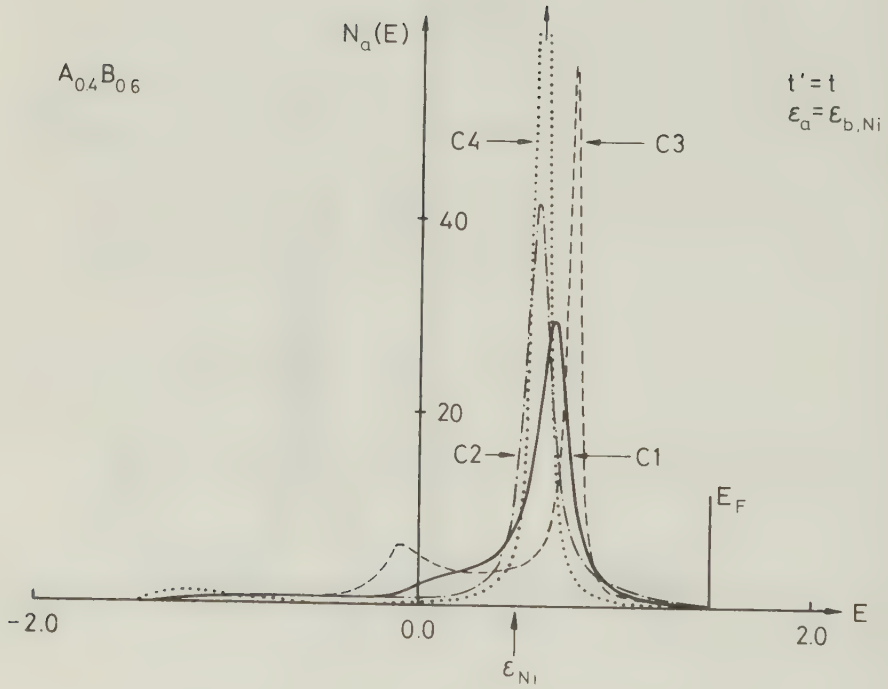

Fig. 14 Local density of states $N_a(E)$ on the adatom for the different substrate configurations C1, C2, C3 and C4. We use $\varepsilon_a=\varepsilon_{Ni,b}$, $t'=t$, $\delta_i=\delta_b$ and the alloy concentration $x=0.4$.

$t_{a,Ni}$ can be easily incorporated in the equation II.25. It is interesting to note, see Fig. 15, that our results for x = 0 reduce to those obtained by Cyrot-Lackmann et al.[9] using the moment expansion method. We conclude from this fact that the local density of states on the adatom does not depend very sensitively on the fine details of the substrate density of states but more on (a) the position (A), (B) or (C) of the adatom, (b) the hopping integral t' between the adatom and the substrate, (c) the local atomic environment (C1), (C2), (C3) or (C4) and (d) the position of ε_a relative to $\varepsilon_{I,i}$ of the substrate.

By alloying we are changing continuously the relative position of ε_a and $\varepsilon_{I,i}$. As a result, in the case of a Ni-adatom on Cu-Ni substrate, the local density of states on the adatom becomes more localized as we go from x = 0 to x = 1. This effect can be best seen for the configuration (C4) when the adatom has four Cu nearest neighbors.

The results obtained for the various adatom positions (A), (B) and (C) may shed some light on the significance of atomic disorder, crystal irregularities, etc. at the surface for chemisorption. The results show that the adatom couples the stronger (see change in the peak width in $N_a(E)$) to the crystal surface the more nearest neighbors it has. Similar results are found if we increase the diffe-

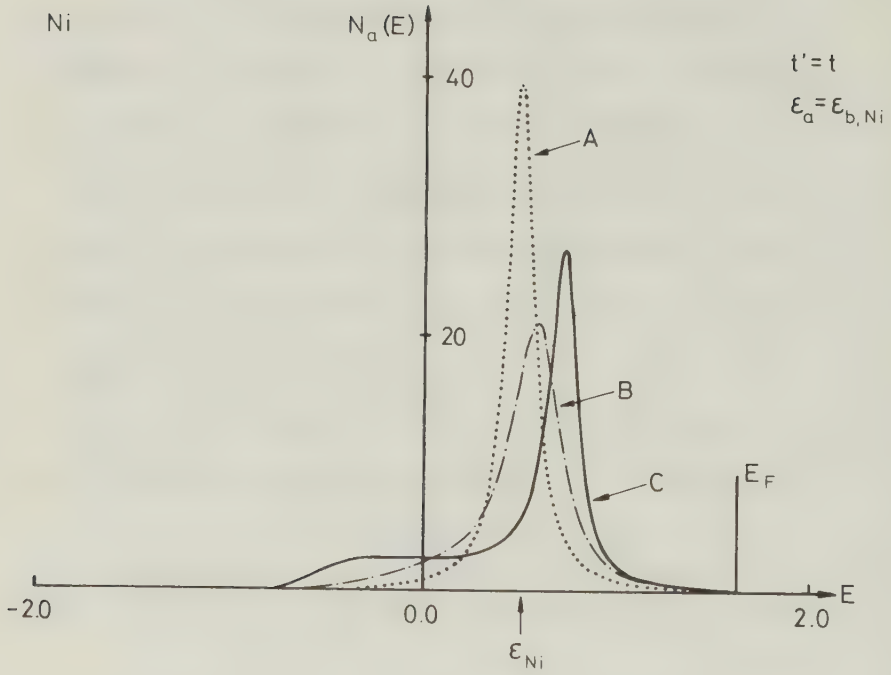

Fig. 15 Local density of states $N_a(E)$ of the adatom on pure Ni for the positions A, B and C. We use $\varepsilon_a=\varepsilon_{Ni,b}$, $t'=t$ and $\delta_i=\delta_b$.

rence ($t'-t$). In Figs. 13 and 14 one observes that for $\varepsilon_a \cong \varepsilon_{Ni}$ the adatom couples more strongly to Ni surface atoms. See, for example, that for configuration (C4) $N_a(E)$ is most similar to $\delta(E-\varepsilon_a)$. We find that only the local atomic environment effects due to nearest neighbors to the adatom are important. The results indicate that cluster effects and segregation at alloy surfaces are important for chemisorption.

To understand the shifts in ε_a, which are shown in Figs. 11 to 14, note that they result primarily from the second term in equation II.23. Consequently, no shift is observed in the adatom position (A) for which only the first term in equation II.23 is present. In contrast, for the adatom positions (B) and (C) the second term is important and leads to shifts in the center of gravity of the adatom density of states. Since more terms of order t^3 occur for the adatom position (C) than for (B), one observes the largest shift in the center of gravity of the local density of states for the adatom position (C).

The binding energy E_B for a chemisorbed atom is given by the energy of the semi-infinite crystal alloy plus the isolated atom minus the energy of the semi-infinite crystal alloy plus the adsorbed atom. This gives for E_B the expresion

$$E_3 = \left[n_a^o \epsilon_a - \tfrac{1}{2} U_a (n_a^o)^2 + \sum_i \int_{-\infty}^{E_F(x)} dE\, E N_i^o(E) - \tfrac{1}{2} \sum_i U_i (n_i^o)^2 \right.$$

$$\left. - \left\{ \int_{-\infty}^{E_F(x)} dE\, E \left[N_a(E) + \sum_i N_i(E) \right] - \tfrac{1}{2} U_a (n_a)^2 - \tfrac{1}{2} \sum U_i (n_i)^2 \right\} \right.$$

$$+ E_B' \qquad \text{II.26}$$

where $n_a^o = \int N_a^o(E)dE$ and $n_a = \int N_a(E)dE$ denote the number of electrons on the adatom, n_a^o refers to the case where no electron charge transfer occurs. U_a denotes the effective intra-atomic Coulomb interction between the electrons on the adatom. The local density of states $N_i^o(E)$ refers to the case where no adatom is present. The local density of states $N_a(E)$ and $N_i(E)$ take into account the interaction between the adatom and the substrate. E_B' is the contribution to E_B which results from the inter-atomic Coulomb interactions and includes the Madelung energy.

If we neglect inter-atomic Coulomb interaction and electron charge transfer between the substrate atoms and the adatom, then the binding energy is given by

$$E_B = n_a \epsilon_a + \int_{-\infty}^{E_F(x)} \sum_i N_i(E)\, E\, dE - \int \left[\sum_i N_i(E) + N_a(E) \right] E\, dE \qquad \text{II.27}$$

In Fig. 16 we show how the adatom binding energy $E_B(x)$ changes as a function of concentration x for different adatom-substrate configurations. The results are obtained assuming that no electron charge transfer occurs. While in general electron charge transfer may be important for determining E_B in the case of CuNi alloy surface electron charge transfer is presumably small and should not affect much the concentration dependence of $E_B(x)$.

For increasing the difference t'-t one finds that E_B increases, but the characteristic dependence of $E_B(x)$ on x remains nearly unchanged. Comparing the results obtained for $E_F(x)$ ($E_F(x) \leq E_{F,Ni}$) calculated from Eq.(II.20) and for $E_F = E_{F,Ni}$ indicate that $E_B(x)$ depends sensitively on $(E_F - \varepsilon_d)$ and hence on electron charge transfer. Notice that $E_F(x) \leq E_{F,Ni}$ is expected if one includes s-electrons in calculating $E_F(x)$ and also from work function data ($\phi_{Ni} - \phi_{Cu} = 0.04$eV). The results shown in Fig. 16 have been obtained assuming $\varepsilon_a = \varepsilon_{Ni,bulk}$.

The curves C4, C1 and C3 with $E_F(x)$ determined self-consistently result if no electron charge transfer occurs. The curve C1 with $E_F = E_{F,Ni}$ implies electron charge transfer and a filling of the Ni d-band at $x \simeq 0.6$. In reality such a transfer may result from the electrons of the adatom as well as from the redistribution of the s-

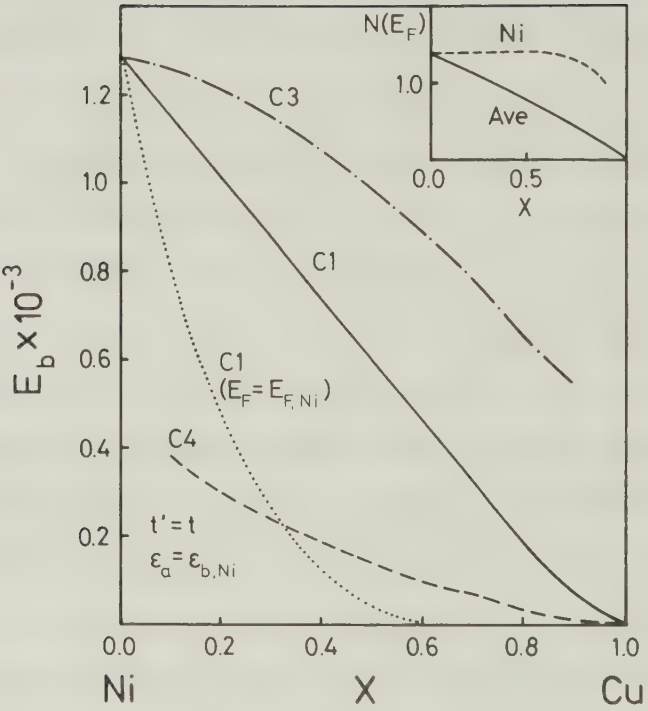

Fig. 16 The binding energy of an adatom as a function of alloy composiiton. We put the adatom in the central position C and assume substrate configurations C1, C2 and C4. We use $\varepsilon_a = \varepsilon_{Ni,b}$, t'=t. All curves are calculated by taking into account the dependence of $E_F(x)$, except C1($E_F = E_{F,Ni}$) which is calculated for constant E_F. The inset shows the average and the Ni surface electron density of states at E_F.

electrons which tend to leak out of the metal. Of course, for a quantitative analysis, electron charge transfer effects should be calculated selfconsistently by taking into account Madelung energies and that energies ε_i depend on n_d.

The dependence of E_B on the concentration x arises from the fact that E_B is mainly determined by the contribution $\int dE(E - \varepsilon_a)N_a(E)$. Consequently, since

$$N_a(E) = n_a\delta(E - \epsilon_a) + x\Delta N_a^{Cu}(E) + (1-x)\Delta N_a^{Ni}(E), \qquad \text{II.28}$$

see Eqs.(II.22) and (II.23), one expects $E_B(x)$ to vary a approximately linear with (1 - x) for an average alloy surface. Here, we denote tha change in $N_a(E)$ due to Cu atoms and Ni atoms by ΔN_a^{Cu} and ΔN_a^{Ni}, respectively. The results obtained for the configuration C4 indicate that $\Delta N_a^{Cu} < \Delta N_a^{Ni}$.

The results obtained for the local atomic environment C3 and C4 indicate that the binding energy of the adatom is strongly determined by the alloy atoms which are nearest neighbours of the adatom.

Assuming that the activation energy E_a for a chemical reaction at the surface is proportional to E_B, then the results for E_B which were obtained for the average

substrate configuration C1 with $E_F(x)$ yield

$$\ln K = a + bx \qquad \text{II.29}$$

which agrees with experiment[51,52]. Here, K is the catalytic activity and a and b are constants.

The results for $E_B(x)$ were obtained without using the rigid band approximation. Similar results for $E_B(x)$ are expected for other transition metal alloys like Ag_xPd_{1-x}, Ag_xRh_{1-x}, etc. For alloys Ni_xPd_{1-x}, Rh_xPd_{1-x}, etc. we expect $E_B(x)$ not to vary very much with x.

If electron charge transfer is important then the Madelung energy could contribute significantly to E_B. Such effects could be calculated directly by extending straightforwardly the theory presented here.

III. SEGREGATION AT THE SURFACE OF TRANSITION METAL ALLOYS.

It has been found experimentally that the catalytic behaviour of alloys is not simply determined by the "sum" of the catalytic properties of their constituents[53,54]. In order to explain this phenomenon more information is needed about the composition of the actual surface exposed to the reacting molecules. There is experimental evidence that one of the factors causing the deviation from additivity is the difference between surface and bulk compositions[19,55]. Using several methods like, work function measurements[19], selective chemisorption[20], electron exited Auger spectroscopy[21] and photon excited electron emission[56], the segregation ar the surface of alloys has been quantitatively determined.

Surface segregation has been studied theoretically so far only within the Bragg-Williams type theory assuming pair-bonds and using concentration independent bond energies as phenomenological parameters[57,59].

In this chapter we present a microscopic theory for the electronic forces responsible for surface segregation. The d-electrons are treated within the tight binding

approximation and the electronic structure at the surface is determined by using the method described in Chapter II. We study for different alloy concentrations the dependence of surface enrichment on electronic alloy parameters like, for example, the difference $\delta = \varepsilon_A - \varepsilon_B$ in d-electron energies of the constituents A and B, the band filling, etc. We show also that solubility changes at the surface.

The surface segregation is calculated by minimizing the total free energy $F(x_1, x_2, \ldots)$ of the crystal with respect to the concentrations $x_1, x_2, \ldots$ of the first, second, ... etc., crystal layers parallel to the surface. We suppose that the crystal consists of a set of planes parallel to the surface and assume a random alloy. Furthermore we neglect vapor effects.

The total Free energy F is minimized with respect to the concentrations $x_1, x_2, \ldots$ such that

$$\sum_i x_i = \text{const.}, \qquad \text{III.1}$$

which expresses that the total number of atoms in the alloy is fixed. Using the Lagrangian multiplier technique one obtains the set of equations

$$\frac{\partial F}{\partial x_i} = \frac{\partial F}{\partial x_h} \qquad i = 1,2,3,.. \qquad \text{III.2}$$

where $\frac{\partial F}{\partial x_b}$ refers to a bulk layer with $x_b = x$.

Eq. (III.2) gives a set of coupled equations determining the surface layers concentrations $x_1, x_2, x_3, \ldots$ etc. One expects that $x_i \neq x_b$ only for the first few atomic layers at the surface.

The free energy

$$F = U - TS \qquad \text{III.3}$$

is now approximately determined as follows. For the entropy we use the lattice contribution

$$S = -k_B N_{\parallel} \sum_i \left[x_i \ln(x_i) + (1-x_i)\ln(1-x_i) \right] , \qquad \text{III.4}$$

where $N_{\parallel}$ denotes the total number of atoms in a layer parallel to the surface, beeing this number the same for all layers. The internal energy U is approximately given by the electronic contribution

$$U = N_{\parallel} \sum_i \int_{-\infty}^{E_F(x)} dE \; E N_i(E, x_1, x_2, \ldots), \qquad \text{III.5}$$

where $N_i(E) = -\frac{1}{\pi} \operatorname{Im} G_i(E)$ is the average electronic densitiy of states in the i-layer. The sum runs over all

layers parallel to the surface. $N_i(E)$ is determined by the average electronic Green's function $G_i(E,x_1,x_2,...)$ of the i-th layer. In terms of the local Green's functions $G_{i,\alpha}$, α=A,B, G_i is given by

$$G_i(E) = x_i G_{i,A} + (1-x_i)G_{i,B} \qquad \text{III.6}$$

for an alloy A_xB_{1-x}. Here, the local electronic Green's function $G_{i,\alpha}(E)$ for electrons on an atom of type α=A,B within the i-th atomic layer is given by

$$G_{i,\alpha}(E) = (E-\varepsilon_{i,\alpha}-\Delta_i)^{-1} \qquad \text{III.7}$$

The renormalization enrgies Δ_i are determined as described in Chapter II.

Results for the surface segregation are shown in Figs. 17, 18 and 19. The numerical results were obtained by taking into account only nearest neighbor interactions assuming t_{ij}=t and using for $\varepsilon_{i,\alpha}$ values refering to the bulk rather than calculating $\varepsilon_{i,\alpha}$ selfconsistently. The latter is certainly necessary if the surface induced electron charge transfer is important.

The numerical results are interpreted as follows. The results shown in Figs. 17 and 18 correspond approximately to an alloy Cu_xNi_{1-x} and show the dependence of surface se-

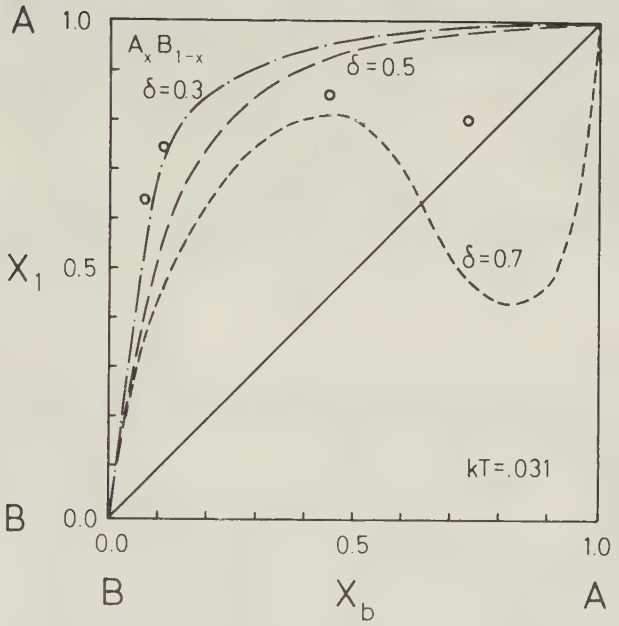

Fig. 17 Results for the surface segregation at the (100) surface of a fcc lattice of an alloy A_xB_{1-x} with $\delta=\varepsilon_A-\varepsilon_B=0.3$, 0.5 and 0.7. $n_A=10$ electrons/atom, $n_B=9.45$ electrons/atom. We express the energy in all the results in units of 0.1227 Ry wnich is half of the Cu d-band width. The dots refer to the experimental results[5]. The curves for x_2 and x_3 show the same behaviour with $x_3\simeq x_b$.

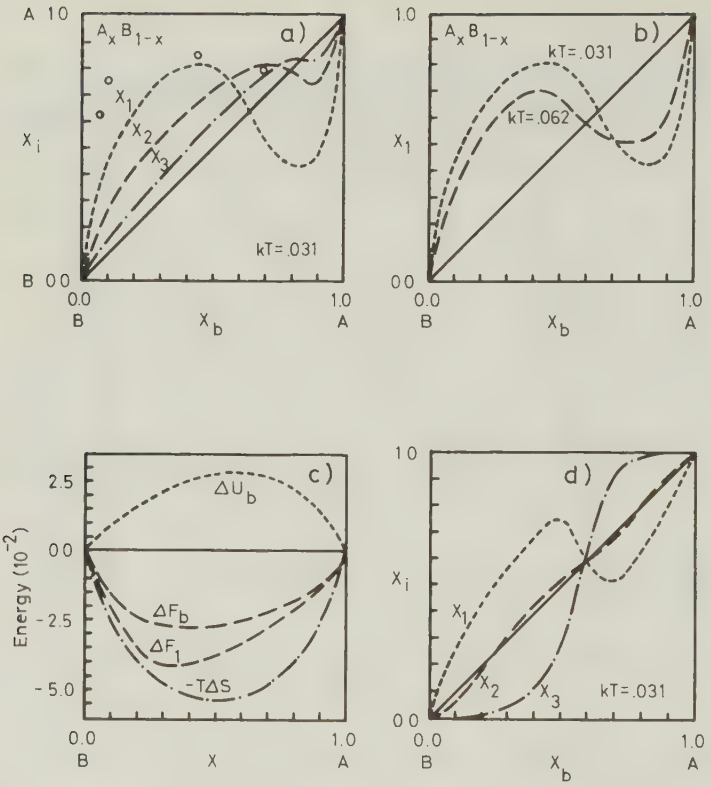

Fig. 18 a) Results for $x_i(x_b)$ for the surface segregation in the first (i=1), second (i=2) and third (i=3) atomic layer parallel to the (100) surface of a fcc lattice. We use $A - B$=0.7, n_A=10 electrons/atom and n_B=9.45 electrons/atom. The values correspond approximately to Cu_xNi_{1-x} alloys. The dots indicate experimental results[5]. b) dependence of the surface segregation on temperature. c) Results for the mixing energies ΔU and the heat of formation ΔF. d) Surface segregation for the case $x_1+x_2+x_3=3x_b$.

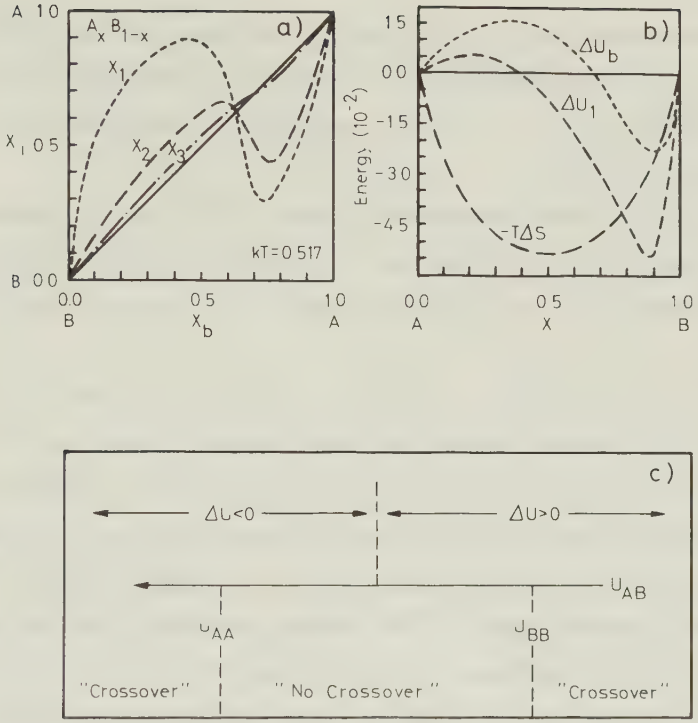

Fig. 19 a) Results for the surface segregation in the (100) direction, $x_i(x_b)$, for the first three layers of a fcc lattice. We use $\varepsilon_A-\varepsilon_B=0.75$, $n_A=7.45$ electrons/atom and $n_B=7.4$ electrons/atom. These values correspond approximately to Ni_xFe_{1-x} alloys. b) Results for the mixing energies at the surface (ΔU_1) and in bulk (ΔU_b). Here we show also the entropy of mixing. c) Illustration of how the crossover behaviour of $x_i(x_b)$ depends on the bond energy U_{AB}.

gregation on $\delta \equiv \varepsilon_A - \varepsilon_B$. We express the enrgy in units of 0.1227 Ry. In particular, the results shown in Fig. 17 seem to agree at least qualitatively with experimental results[6,60,61].

In contrast to previous theories[57-59] which are restricted to alloys which can be treated by the rigid-band approximation, we obtain in general a crossover of the curves x_i vs x_b.

However, this crossover is in general expected on energetic grounds if the A-B bond energy U_{AB} does not fall between the bond energies U_{AA} and U_{BB} refering to A-A and B-B bonds, respectively. Then the free energy can be lowered by minimizing the number of A-B bonds enriching the surface with B atoms in the A-rich alloys and with A atoms in the B-rich alloys. This crossover behaviour for x_i can also be obtained by using the Bragg-Williams type theory for surface segregation[57-59] if $U_{AB} \lesseqgtr (U_{AA}, U_{BB})$. If U_{AB} lies in between U_{AA} and U_{BB}, then $x_i(x_b)$ shows no crossover. This is illustrated in Fig. 19(c). This behaviour is also obtained within our microscopic theory for certain mixing energies

$$\Delta U(x) = U(x) - xU(1) - (1-x)U(0) \qquad \text{III.8}$$

A crossover is expected for alloys with mixing energies

$\Delta U > \Delta U_o \equiv x(1-x)|U_{AA}(1)-U_{BB}(0)|$. The results shown in Fig. 17 for $\delta_1=0.7$ and $\delta_2=0.5$ support these conclusions since we estimated $\Delta U(\delta_1) > \Delta U_o > \Delta U(\delta_2)$.

We find that the crossover $x_i(x_b)$ occurs for such x_i for which ΔF_i, which denotes the contribution to the energy of mixing ΔF due to the i-th layer, has a minimum. This is physically plausible since the ΔF_i does not change much when x_i varies.

The results show that surface segregation is essentially limited to the first three atomic layers at the surface, and that it decreases for increasing temperature, as it is shown in Fig. 18(b). Also, since for increasing temperature $\Delta F(\ldots x_i, \ldots)$ is more determined by the term $-T\Delta S$, which has a minimum at $x=0.5$, one expects in cases when a crossover occurs in $x_i(x_b)$ that for increasing temperature the concentration at which the crossover occurs approaches 0.5.

In the case of surface segregation in semi-infinite slabs, the bulk acts like a reservoir of atoms and consequently segregation may involve exchange of atoms between this bulk reservoir of atoms and atoms in layers near the surface. In thin films slabs the atomic redistribution accompanying segregation can be only between a finite number of atomic layers. In the case of a thin film of three layers, the equations III.1 and III.2 reduce to

$$x_1 + x_2 + x_3 = 3x_{av} \text{ and } \frac{\partial F}{\partial x_1} = \frac{\partial F}{\partial x_2} = \frac{\partial F}{\partial x_3}. \qquad \text{III.9}$$

In Figs. 18(d), 20 and 21 we show results for the segregation occuring in thin films which were obtained by using the boundary conditions $x_1+x_2=2x_{av}$ and $x_1+x_2+x_3=3x_{av}$, corresponding to thin films on the top of a metal with only one free surface and where the metalic substrate of the film does not participate in the atomic exchange leadin to segregation (see, for example, Cu-rich Cu_xNi_{1-x} film on Ni). For the case $x_1+x_2+x_3+x_4=4x_{av}$ the segregation trend indicated by the comparison of Figs. 20 and 21 continues. For all these calculations we have used parameters corresponding to Cu_xNi_{1-x} alloys.

In Figs. 22 and 23 we show results for the segregation occuring in thin films of 4 and 6 atomic layers, respectively. The results were obtained by using the conditions $x_1+x_2=2x_{av}$, $x_2=x_3$, $x_1=x_4$ and $x_1+x_2+x_3=3x_{av}$, $x_3=x_4$, $x_2=x_5$, $x_1=x_6$, respectively.

In Fig. 24 we present results illustrating the dependence of segregation on the boundary condition $\sum x_i=Nx_{av}$.

Our theory can also be used to determine the behaviour of transition metal atoms deposited on a transition metal. One observes experimentally, for example, that Cu-atoms deposited on a Ag- substrate are not uniformly chemisorbed

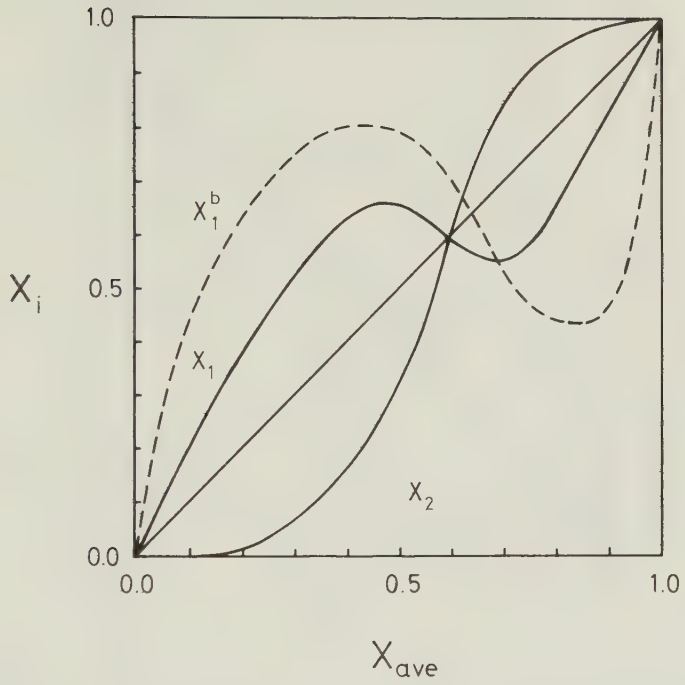

Fig. 20 Results for the surface segregation in the first and second layer of a thin film on the top of a metal. The surface geometry is that of a (100) surface of a fcc lattice. We use the condition $x_1+x_2=2x_{ave}$ and the parameters $\varepsilon_A-\varepsilon_B=0.7$, $n_A=10$ electrons/atom and $n_B=9.45$ electrons/atom. The results for the first layer concentration in the case of a semi-infinite crystal is denoted by x_1^b.

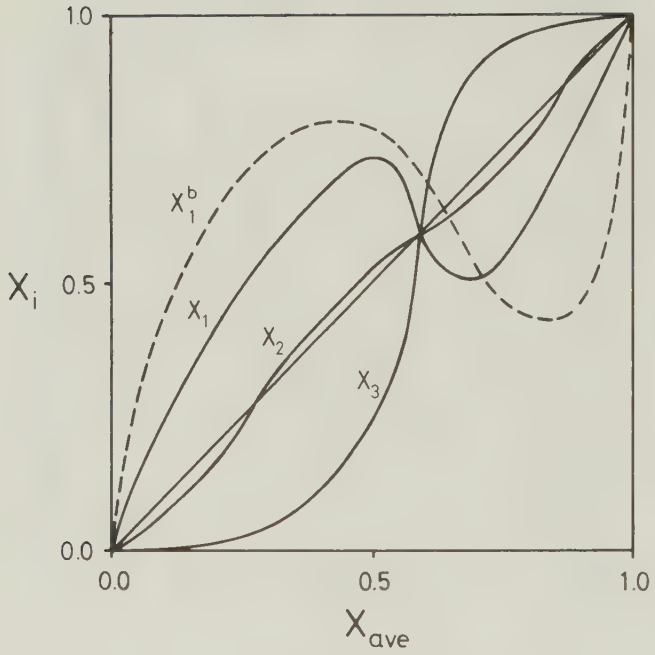

Fig. 21 Surface segregation in a three-layer thin film on top of a metal. We use the condition $x_1+x_2+x_3=3x_{ave}$. The parameters used are the same as in Fig. 20.

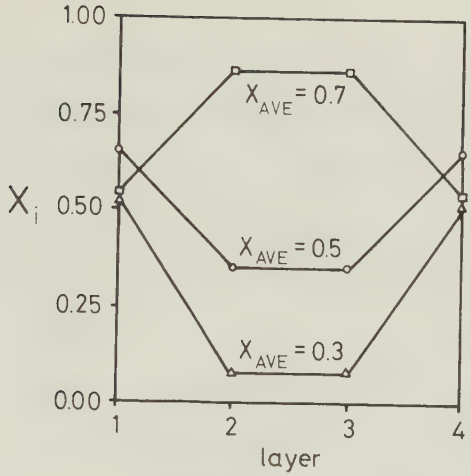

Fig. 22 Composition profile for different average concentrations in a four-layer thin film for $x_1=x_4$ and $x_2=x_3$. The parameters are the same as in Fig. 20.

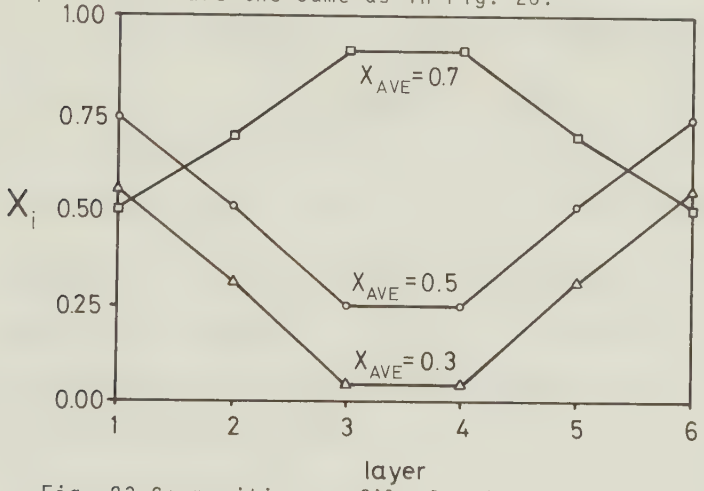

Fig. 23 Composition profile for different average concentrations ia a six-layer thin film for $x_1=x_6$, $x_2=x_5$ and $x_3=x_4$. The parameters are the same as in Fig. 20.

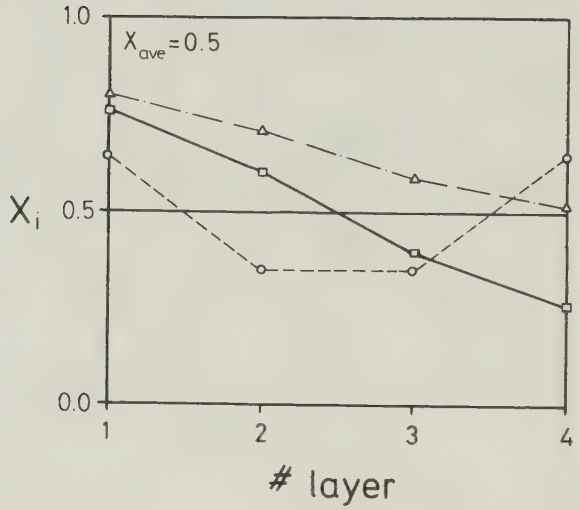

Fig. 24 Composition profile for a) four-layer thin film with both surfaces free (circles), b) a four-layer thin film on a metal surface (squares) and c) semi-infinite crystal (triangles). The parameters used are the same as in Fig. 20.

but tend to form bulk clusters on the Ag-surface. If Ag-atoms are deposited on a Cu-surface, they do not cluster but form superstructures[62]. Applying our theory, these observations can be explained as follows. The behaviour of the deposited atoms is determined by the heat of mixing $\Delta F=\Delta U-T\Delta S$. According to our results on segregation, Cu and Au segregate at the surface. Thus, Cu-atoms will stay at the surface and the concentration of Cu-atoms in the surface layers of Ag is negligible. Within our gas-approximation for the entropy contribution ΔS to ΔF is not sufficient to cause mixing. Then, due to the fact that one finds $U_{Cu-Cu}<U_{Cu-Ag}<U_{Ag-Ag}$ for the pair bond energies, we obtain that ΔU is minimal if the Cu-atoms for energetically favourabla Cu-Cu bonds. Moreover, bulk Cu-Cu bonds are more favourable than those within a Cu monolayer. Consequently, islands of bulk Cu-clusters are formed. This explains the experimental observation. In the case of Ag-atoms at the surface of Cu, we again have that due to surface segregation there is approximately no mixing of Ag and Cu at the surface. In this case ΔU is minimal if as many Cu-Ag bonds as possible are formed, thus explaining the absence of bulk clustering of Ag-atoms at the surface of Cu and the formation of a monolayer of Ag-atoms. Superstructures are formed in order to minimize the repulsive Ag-Ag interaction[63,64]. We expect superstructures if

the mean distance between the chemisorbed Ag-atoms becomes smaller than the range of Ag-Ag interaction. Note, these results occur for strong segregation. If mixing of Ag- and Cu-atoms would occur in the substrate, then this weakens the tendency towards forming clusters and superstructures, respectively. Generally, in the case of strong segregation we expect islands of bulk clusters for those transition metal atoms which have a higher binding energy than the transition metal atoms of the substrate. For example, Ni-atoms on top of a Cu-substrate should form clusters. Note, our arguments on bulk cluster formation at the surface apply only as long as surface segregation is dominant which limits the size of the deposited bulk clusters.

Figure 19 shows results for an alloy which roughly corresponds to Ni_xFe_{1-x}. Notice that for such an alloy one obtains a larger surface segregation than for Cu_xNi_{1-x} type alloys. This is expected since the difference is surface tensions $(\gamma_A-\gamma_B)$ which approximately causes the surface segregation [65] is larger for Fe and Ni than for Ni and Cu. Notice that $f(x)=\Delta U/(1-x)x$ is a strong function of x, and therefore surface segregation in such an alloy can not be treated within the Bragg-Williams-type theory with concentration independent bond energies.

Comparison of the results in Figs. 17, 18 and 19 demostrates the dependence of the surface segregation on the

difference $\delta=\varepsilon_A-\varepsilon_B$ in d-electron energies and on the filling of the d-band. In all cases one finds for small concentrations x a surface enrichment with those atoms which have the larger number of d-electrons. In general our theory yields for alloys $A_{1-x}B_x$ the following behaviour with respect to surface segregation. If n_A, n_B 5 and $n_A<n_B$, then in B-rich alloys surface segregation consists in an enrichment of A-atoms, while for n_A, n_B 5 and $n_A>n_B$ surface segregation consists of an enrichment of B-atoms in A-rich alloys. This is in agreement with experimental results[66,67] on $Pd_{1-x}Ag_x$, $Pd_{1-x}Au_x$, $Ni_{1-x}Au_x$ and $Pt_{1-x}Ag_x$, for example, where for small concentrations x an enrichment of the noble metal atoms is observed at the surface.

It would be of interest to study also the dependence of surface segregation on atomic volume, surface relaxation and surface roughness. This could be done within our theory by assuming different hopping integrals t_{AA}, t_{AB} and t_{BB} in $A_{1-x}B_x$ alloys. The increase in elastic (strain) energy in alloys with different atomic volume Ω_A and Ω_B has been estimated[68] to be of the order of 0.1-0.2 eV and will cause (at least in harmonic lattices) a segregation of solute atoms to the surface. This (elastic) driving force for segregation may be neglected, however, if $0.1\ eV \ll |\gamma_A-\gamma_B|$.

Our theory could be also extended to study the influence of chemisorbed atoms and molecules on the surface segregation. Such a chemisorbed induced segregation[57,69,70] favors an enrichment of such atoms at the surface which establish stronger chemisorption bonds. For example, in Cu_xNi_{1-x} alloys the surface segregation is reduced due to chemisorbed atoms or molecules which essentially couple only to Ni-atoms[70].

The effect of electron charge transfer on surface segregation is also of interest. This can be included in our theory by calculating $\varepsilon_{i,\alpha}=\varepsilon^{o}_{i,\alpha}+U_{\alpha}n_{i,\alpha}$ self-consistently and by adding the Madelung energy[71] U_M to F. If the electron charge transfer results from a s→d electron redistribution, then it amounts simply to a d-band filling. Assuming for simplicity an alloy A_xB_{1-x} where d states of the A-atoms are filled, then we expect due to s→d charge transfer an increase in surface segregation if $n_{d,B} \leq 5$ and a decrease if $n_{d,B} \gtrsim 5$ in accordance with the dependence of surface tension on n_d

At sufficient high temperatures the contribution to the free energy F due to the (vibrational) motion of the atoms play a role if the Debye temperature $\Theta_{D,A}$ is very different from $\Theta_{D,B}$ or the self-diffusion of A-atoms is very different from that of the B-atoms.

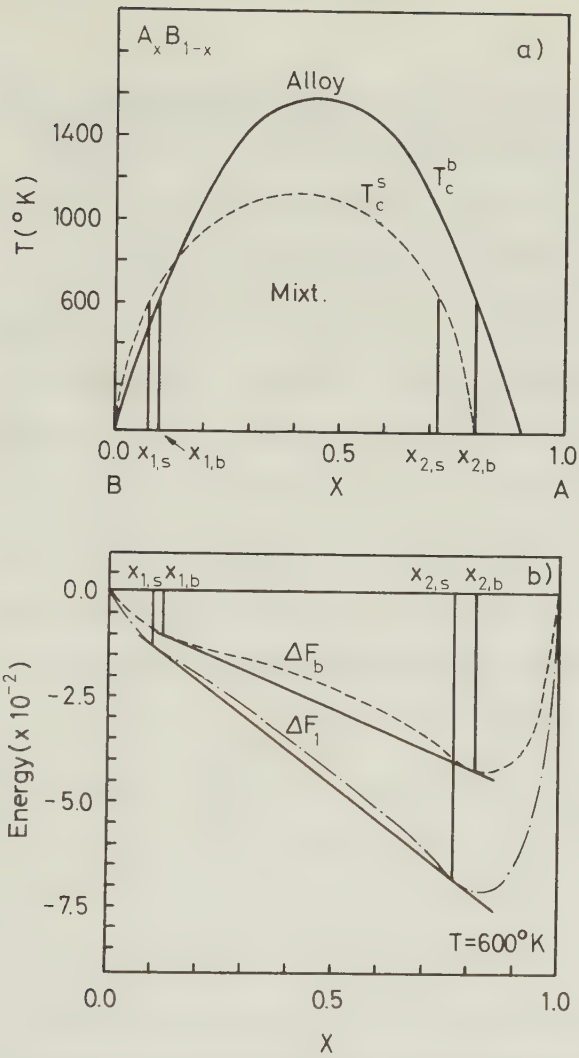

Fig. 25 a) Illustration of the change in the miscibility gap at the surface of an alloy corresponding to the same alloy parameters as in Fig. 19. T_C is the critical temperature above which homogeneous alloys (solutions) occur. The critical concentrations are obtained as indicated in b).

An important problem related to surface segregation is how the surface changes the solubility range of an alloy A_xB_{1-x}. In Fig.25 we illustrate for an alloy corresponding roughly to Ni_xFe_{1-x} alloys how the surface affects the solubility or the stability of homogeneous solutions, respectively. One expects in general that the critical temperature T_C for homogeneous solutions is smaller at the surface than in bulk. Since $T_C=x(1-x)f(x)$ one expects of course at the surface where $x_1 \neq x_b$ due to surface segregation that $T_C^s \neq T_C^b$. We obtain in general $T_C^s(x)<T_C^b(x)$, since $0<\Delta U_s<\Delta U_b$ holds over the concentration range where $\Delta U>0$. Also note that we obtain at the surface a change in the critical concentrations $x_{C,s}$ and $x_{C,b}$ for homogeneous alloys.

IV. SELECTIVE CATALYTIC BEHAVIOUR OF THE Cu-Ni ALLOY SURFACE.

Here we show that the selective catalytic behaviour of Cu_xNi_{1-x} alloy surface can be understood in terms of a simple model. Using this model the concentration dependence of the catalytic activity is calculated taking into account surface segregation and local atomic environment effects.

It has been observed[5, 22, 23] that the catalytic activity and selectivity of alloy surfaces can change drastically when the alloy composition is changed. As an example, the concentration dependence of the activity of cyclopropane hydrogenation and hydrogenolysis at the surface of Cu-Ni is shown in Fig. 26 [23]. It has been suggested that the reduction of the hydrogenolysis reaction at the surface of Cu_xNi_{1-x} alloys observed for increasing Cu concentration results from the fact that the cracking of C-C bonds required for the chemical reaction is due to C-atoms chemisorbed such that they are surrounded by 4 Ni-atoms as nearest-neighbors[22]. It is shown in the following that this simple geometrical hypothesis is not sufficient to explain the observed concentration dependence of the catalytic activity. For example, it is important to include surface segregation to explain the concentration dependence of the

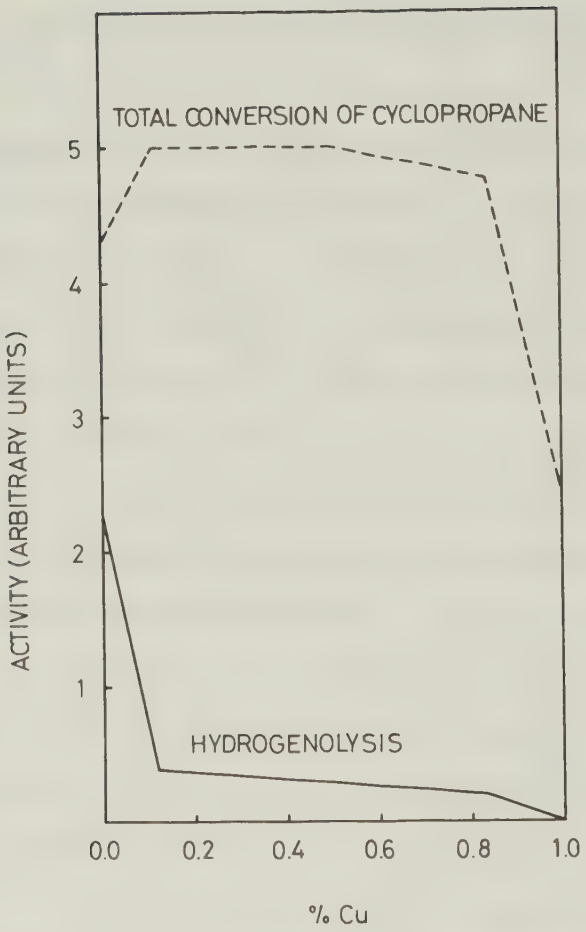

Fig. 26 Experimental results for the activities of Cu_xNi_{1-x} alloy catalists for hydrogenolysis and total conversion of cyclopropane.

chemical reaction.

In the following we present a simple model calculation for the activation energy a(x). For a cracking reaction to occur, we assume that the binding energy E_B of the chemisorbed C-atoms has to be large enough to break the C-C bonds. Hence, to explain a(x) we assume that the activation energy a(x) is proportional to the average binding energy of the chemisorbed C-atoms, $a(x)=\text{const}\ E_B(x)$, and that a minimum value for E_B is needed for hydrogenolysis or cracking reactions to occur. For simplicity we study the cracking reactions at the (100) surface plane of a Cu_xNi_{1-x} alloys. The binding energy is then calculated from

$$E_B(x_S) = \sum_{i=0}^{4} P_i(x_S) E_{B,i}(x_S) \ , \qquad \text{IV.1}$$

where $E_{B,i}(x_S)$ is the binding energy of the chemisorbed (C-) atom at a surface site with i Cu-atoms and (4-i) Ni-atoms as nearest neighbors and for a Cu concentration x_S. Note, in the case of segregation x_S will be different from the bulk concentration x. $P_i(x_S)$ denotes the probability to find a chemisorbed atom with i Cu-nearest-neighbors and is given by the binomial distribution

$$P_i(x_S) = \frac{4!}{i!(4-i)!}\, x_S^i (1-x_S)^{4-i} . \qquad \text{IV.2}$$

The binding energies $E_{B,i}(x_S)$ are calculated as described

in Chapter II C). Assuming for the chemisorbed atom the central position shown in Fig. 27, one obtains for $E_{B,i}(x)$ the results shown in the same figure. Using these results and equation IV.1 we obtain for $E_B(x)$ and then for a(x) the results shown in Fig. 28. The sensitive dependence of E_B and a on x suggests that surface segregation may affect a(x) significantly. Therefore, we show in Fig. 29 the results obtained for a(x) by determining for a given composition x the quantities P_i and $E_{B,i}$ with

$$x_S = (1-x_S^o)\alpha_1 + x_S^o. \qquad \text{IV.3}$$

Here, α_1 is the first shell short range order parameter and $x_S^o = x_S^o(x)$ is the surface concentration which differs from the bulk concentration due to surface segregation. We use for α_1 values proposed by Robbins et al.[78] to explain the distribution of local magnetic moments in Cu_xNi_{1-x} alloys. For $x_S^o(x)$ we take the results obtained in Chapter III. Note, $\alpha_1=0$ yields nearly the same results as shown in Fig. 29.

In conclusion, we have shown that in order to explain the catalytic activity for cracking reactions at the surface of Cu_xNi_{1-x} alloys one has to take into account local environment effects and surface segregation. Cracking reactions will occur at chemisorption sites of C-atoms surrounded by four Ni-, three Ni- and two Ni-atoms. Adatoms sur-

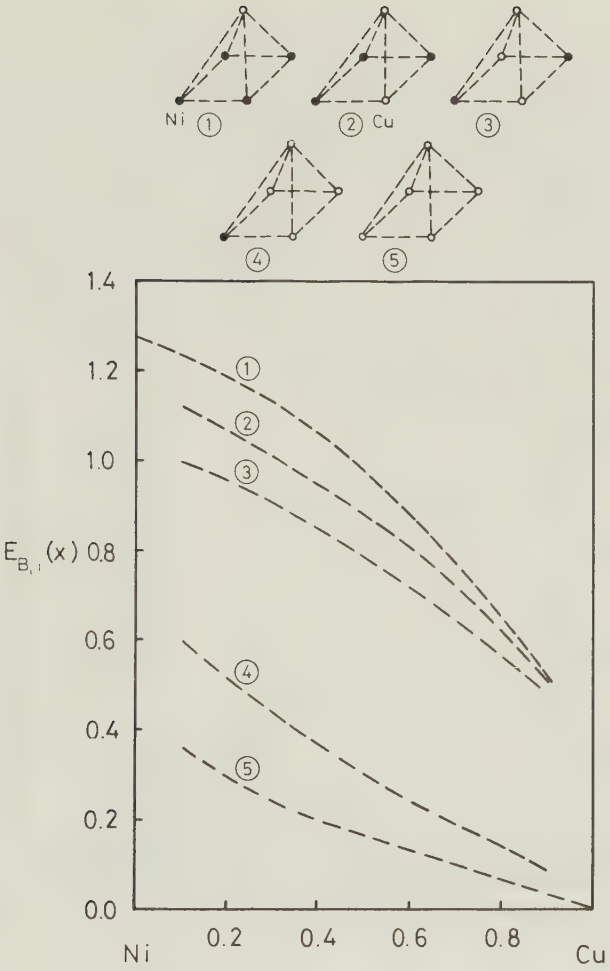

Fig. 27 Concentration dependence of the binding energy of an adatom chemisorbed in the central position. The curves refer to the different configurations.

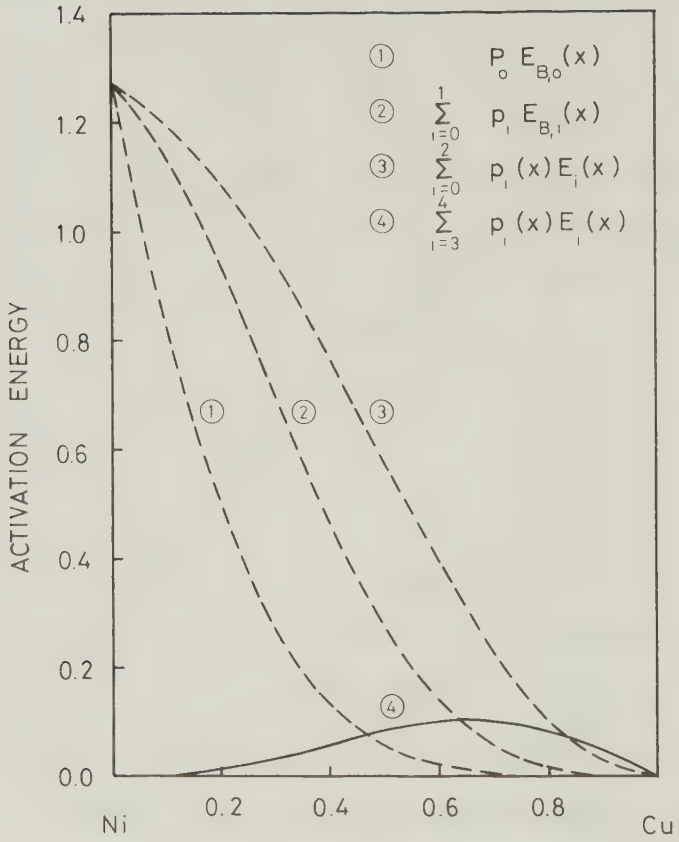

Fig. 28 Concentration dependence of the activation energy. The curves are obtained taking into account the contributions ahown in the upper part. No segregation is included.

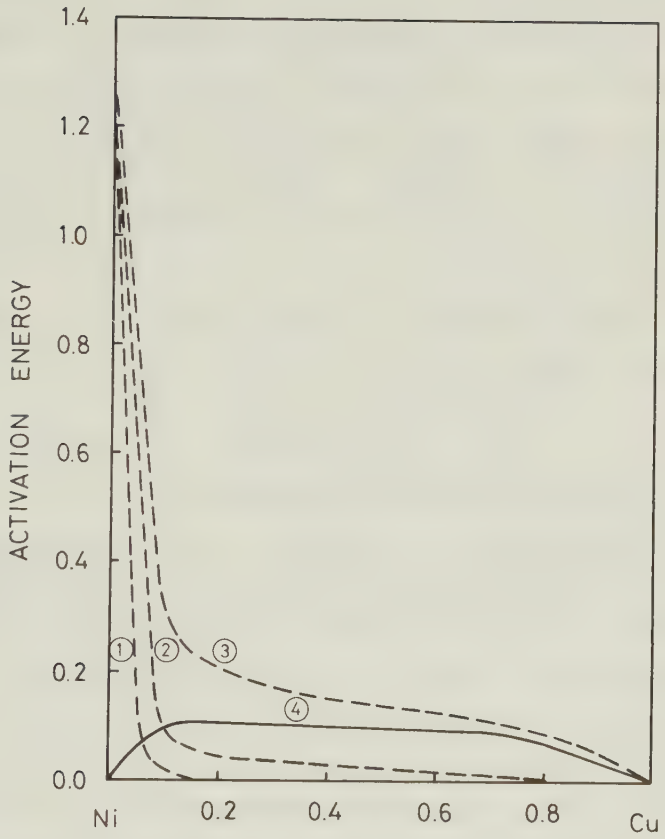

Fig. 29 Concentration dependence of the activation energy. The curves are obtained as in Fig. 28. Here, segregaiton is taken into account.

rounded by one or no Ni-atoms have a binding energy which is too low to break the C-C bonds. However, on the other hand these adatom configurations are favorite sites for hydrogenation processes which do not require breaking of C-C bonds and will give aditional sites for non destructive reactions. If N_C and N_{NC} are the number of sites used for craking and non-craking reactions, we can write

$$N_C = N_C^o \, P_C(x_S) \qquad \text{IV.4}$$

and

$$N_{NC} = N_{NC}^o \, P_{NC}(x_S) + N_C^o \, P'_{NC}(x_S), \qquad \text{IV.5}$$

where N_C^o and N_{NC}^o are the number of sites used for destructive and non-destructive processes in pure Ni. $P_C(x_S)$ and $P_{NC}(x_S)$ are the probabilities to find a destructive or non-destructive site, respectively. The second term of the rigth hand side of equation IV.5 is the contribution to the non-destructive sites coming from the original craking sites transformed in non-craking sites upon alloying. P'_{NC} and P_{NC} are different since the adatom positions for destructive and non destructive processes are different. In Fig. 29 (curve 4) we show the contribution to the activation energy of hydrogenoliysis resulting from the convertion of destructive to non-destructive sites. Since the binding energy

of an adatom in the central position (craking position) is higher than in the top position (non-craking position) one expects that the ratio N_C/N_{CN}, and therefore a_C/a_{NC}) will increase for decreasing temperature.

Notice that our calculation for $E_{B,i}$ refer to a model adatom and not to a realistic adsoption of C-atoms. However, it seems a reasonable assumption that $E_{B,i}(x)$ for real C-atoms will exhibit the same environment dependence as obtained in our model calculation. Furthermore, one should also notice that chemisorbed atoms can influence surface segregation[57,59,70] which we have neglected. For low adsorbate coverage the interaction between adatoms and substrate con be ignored. Our model calculation show that local environment effects are important for understanding selective catalysis at transition-metal alloy surfaces.

V. ORDER-DISORDER PHASE TRANSITION AT THE SURFACE OF BINARY ALLOYS.

Experimentally it has been found that in ordered alloys, like Cu_3Au, the order-disorder phase transition is affected by the surface[24]. There are also experimental results on segregation in ordered alloys at temperatures higher than than the order-disorder transition temperature[72]. However, no experimetal results on surface order-disorder transitions as well as quenching of the order state at the surface and the effect of segregation in the order-disorder transition are available.

In this chapter we present a Bragg-Williams type theory for the effect of the surface on order-disorder phenomena. The effect of surface segregation on atomic ordering is taken into account. It is shown that within the first few atomic layers at the surface the atomic ordering is strongly reduced due to the surface. This agrees with the experimental results for Cu_3Au. We show that the effect of the surface on the order-disorder transition is different for different surface geometry. Surface segregation has a strong effect on atomic ordering. As a result of surface segregation the order parameter in the vicinity of the surface can be strongly reduced and might even disappear at some temperature below the transition temperature.

A simple electronic theory for the order-disorder phase transition at the surface is presented in Appendix D.

In the following we study atomic ordering at the surface of a fcc lattice for A_3B alloys. The lattice is decomposed into planes parallel to the surface. Then the atomic order parameter η_i for the i-th plane away from the surface is defined by

$$\eta_i = p^A_{\alpha,i} - p^A_{\beta,i}, \qquad V.1$$

where $p^A_{\alpha,i}$ and $p^A_{\beta,i}$ are the probabilities to find an A atom in the i-th plane in the α and β sublattice, respectively. Note, in the case of a fcc lattice and A_3B alloys the α sublattice consists of all face-centered sites and the β sublattice of all the corner sites of the fcc lattice. This is illustrated in Fig. 30. Noting that $N_{\alpha,i}p^A_{\alpha,i}+N_{\beta,i}p^A_{\beta,i}=x_iN_i$ where $N_{\alpha,i}$ and $N_{\beta,i}$ are the numbers of α and β lattice sites in the i-th layer with N_i atoms and concentration x_i of A atoms, one finds that

$$p^A_{\alpha,i} = \frac{\eta_i+(N_i/N_{\beta,i})x_i}{1+N_{\alpha,i}/N_{\beta,i}}$$

and

$$p^A_{\beta,i} = \frac{N_i}{N_{\beta,i}}\cdot x_i - \frac{\eta_i+(N_i/N_{\beta,i})x_i}{1+N_{\beta,i}/N_{\alpha,i}} \quad .$$

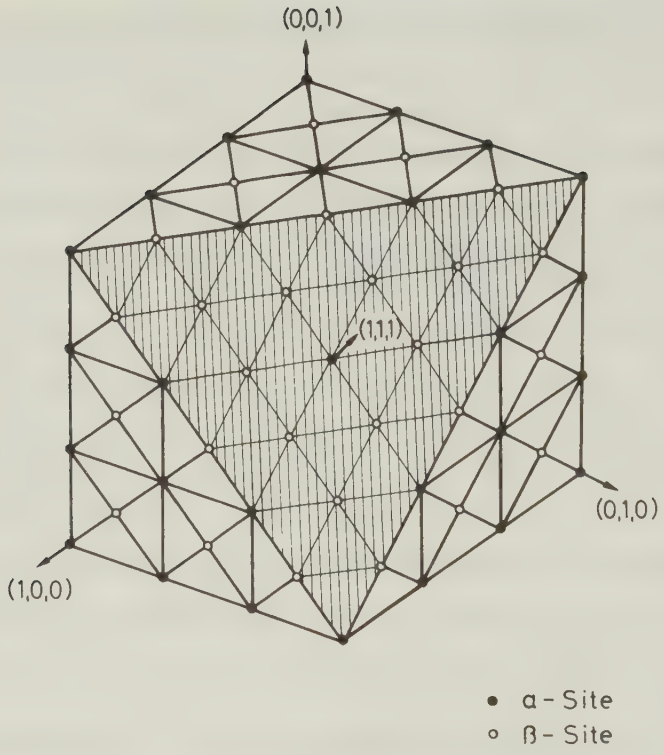

Fig. 30 α- and β-sublattices of the considered fcc lat lattice.

Then, $p^B_{\alpha,i}$ and $p^B_{\beta,i}$ can be obtained from $p^A_{\alpha,i}+p^B_{\alpha,i}=1$ and $p^A_{\beta,i}+p^B_{\beta,i}=1$. The equilibrium values for x_i and n_i are then determined by minimizing the free energy

$$F = U - TS, \qquad V.2$$

with respect to x_i and n_i. This yields the equations

$$\frac{\partial F}{\partial n_i} = 0 \qquad V.3$$

and

$$\frac{\partial F}{\partial x_i} = \frac{\partial F}{\partial x_b}. \qquad V.4$$

Here, x_b is the average concentration of A atoms in the bulk. The equations will be evaluated by using for the entropy S the expression $S=\sum_i S_i$, where S_i is the contribution due to the i-th layer and is given by

$$S_i = k\ln\left(\frac{N_{\alpha,i}!}{N^A_{\alpha,i}!N^B_{\alpha,i}!}\right)\left(\frac{N_{\beta,i}!}{N^A_{\beta,i}!N^B_{\beta,i}!}\right).$$

Similarly, by using the Bragg-Williams approximation the internal energy U is written $U=\sum_i (U_i^{(1)}+U_i^{(2)})$, where $U_i^{(1)}$ and $U_i^{(2)}$ are the contributions due to the i-th layer which result from nearest and next-nearest- neighbor interactions.

In the Appendix C these energies $U_i^{(1)}$, $U_i^{(2)}$ are determined explicitly.

A. (111) surface

In the following we evaluyte equations V.3 and V.4 for the case of a (111)surface plane. Then one finds

$$N_{\alpha,i} = \frac{3}{4} N_i \quad \text{and} \quad N_{\beta,i} = \frac{1}{4} N_i ;$$

and

$$\begin{aligned} p^A_{\alpha,i} &= x_i + \frac{1}{4}\eta_i , \\ p^B_{\alpha,i} &= 1-x_i - \frac{1}{4}\eta_i , \\ p^A_{\beta,i} &= x_i - \frac{3}{4}\eta_i , \end{aligned} \qquad \text{V.5}$$

and

$$p^B_{\beta,i} = 1-x_i + \frac{3}{4}\eta_i .$$

Using now the expressions for S_i, $U_i^{(1)}$ and $U_i^{(2)}$ one obtains from equation V.3 the coupled set of equations

$$\frac{W^{(1)}}{RT}\left(\eta_1 + \tfrac{1}{2}\eta_2\right) - \frac{W^{(2)}}{kT} 3\eta_2 = 3 \ln \frac{(x_1 + \frac{1}{4}\eta_1)(1-x_1+\frac{3}{4}\eta_1)}{(1-x_1-\frac{1}{4}\eta_1)(x_1-\frac{3}{4}\eta_1)} ,$$

$$\frac{W^{(1)}}{kT}\left(\eta_2 + \tfrac{1}{2}\eta_1 + \tfrac{1}{2}\eta_3\right) - \frac{W^{(2)}}{kT} 3(\eta_1+\eta_3) = 3 \ln \frac{(x_2+\frac{1}{4}\eta_2)(1-x_2+\frac{3}{4}\eta_2)}{(1-x_2-\frac{1}{4}\eta_2)(x_2-\frac{3}{4}\eta_2)} ,$$

.
.
.

and from equation V.4 the coupled set of equations

$$\frac{W^{(1)}}{kT}(6x_1+3x_2-12x_b)+\frac{3}{2kT}\left[W^{(1)}-(U_{BB}^{(1)}-U_{AA}^{(1)})\right]+\frac{6W^{(2)}}{kT}(x_2-2x_b)$$

$$+\frac{3}{kT}\left[W^{(2)}-(U_{BB}^{(2)}-U_{AA}^{(2)})\right]=\frac{3}{2}\ln\frac{(x_b+\frac{1}{4}\eta_b)^3(x_b-\frac{3}{4}\eta_b)(1-x_1-\frac{1}{4}\eta_1)^3(1-x_1+\frac{3}{4}\eta_1)}{(1-x_b-\frac{1}{4}\eta_b)^3(1-x_b+\frac{3}{4}\eta_b)(x_1+\frac{1}{4}\eta_1)^3(x_1-\frac{3}{4}\eta_1)},$$

$$\frac{W^{(1)}}{kT}(6x_2+3x_1+3x_3-12x_b)+\frac{6W^{(2)}}{kT}(x_1+x_2-2x_b)$$

$$=\frac{3}{2}\ln\frac{(x_b+\frac{1}{4}\eta_b)^3(x_b-\frac{3}{4}\eta_b)(1-x_2-\frac{1}{4}\eta_2)^3(1-x_2+\frac{3}{4}\eta_2)}{(1-x_b-\frac{1}{4}\eta_b)^3(1-x_b+\frac{3}{4}\eta_b)(x_2+\frac{1}{4}\eta_2)^3(x_2-\frac{3}{4}\eta_2)},$$

.
.
.

V.7

These equations determine x_i and η_i. The energies of unmixing $W^{(1)}$ and $W^{(2)}$ which refer to nearest- and overnearest-neighbor bond are given by $W^{(i)}=2U_{AB}^{(i)}-U_{AA}^{(i)}-U_{BB}^{(i)}$, i=1,2. Notice that if segregation is absent or neglected then all $x_i=x_b=0.75$ and equations V.6 simplify to

$$\frac{W^{(1)}}{kT}(\eta_1+\tfrac{1}{2}\eta_2)-\frac{W^{(2)}}{kT}3\eta_2=3\ln\left[1+\frac{16\eta_1}{3(1-\eta_1)^2}\right],$$

$$\frac{W^{(1)}}{kT}(\eta_1+\tfrac{1}{2}\eta_1+\tfrac{1}{2}\eta_3)-\frac{3W^{(2)}}{kT}(\eta_1+\eta_3)=3\ln\left[1+\frac{16\eta_2}{3(1-\eta_2)^2}\right],$$

.
.
.

B. (100) surface

In the (100) direction there are two types of different planes. There are planes of type 1 with equal number of α and β sites, such that $N_{\alpha,i}=N_{\beta,i}=\frac{1}{2}N_i$. The other planes of type 2 contain only α sites. Thus, one can define order parameters

$$p^A_{\alpha,i} = x_i + \frac{1}{2}\eta_i, \qquad p^A_{\beta,i} = x_i - \frac{1}{2}\eta_i,$$
$$p^B_{\alpha,i} = 1-x_i - \frac{1}{2}\eta_i \quad \text{and} \quad p^B_{\beta,i} = 1-x_i + \frac{1}{2}\eta_i \qquad \text{V.9}$$

for the planes of type 1. For the planes of type 2 one has

$$p^A_{\alpha,i\pm1} = x_{i\pm1} \quad \text{and} \quad p^B_{\alpha,i\pm1} = 1-x_{i\pm1}$$

If one now subdivides the lattice into these planes parallel to the (100) surface, one has to allow interchange of atoms between adjacent planes in the way to properly describe the order. That is, the concentrations x_1^b, x_2^b refering to the two kinds of planes are functions of the temperature. In the complete ordered case the concentrations will be $x_1^b=0.5$ and $x_2^b=1$, respectively, and in the disordered situation the concetrations will be 0.75 everywhere. To calculate for the bulk x_1^b, x_2^b, and η_b as a function of

of T we use the equations

$$\frac{\partial F}{\partial x_1^b} = \frac{\partial F}{\partial x_2^b} , \quad \frac{\partial F}{\partial n_b} = 0,$$

with

$$x_1^b + x_2^b = 2x_b$$

The solution of these equations are shown in Fig. 31. This gives a linear dependence of the concentrations on n_b:

$$x_1^b = \frac{3}{4} - \frac{1}{4}n_b \quad \text{and} \quad x_2^b = \frac{3}{4} + \frac{1}{4}n_b$$

In the case that the surface plane is of type 1 the equations determining n_{2i-1} and x_i are

$$\frac{4w^{(1)}}{kT}\eta_1 - \frac{2w^{(2)}}{kT}(4\eta_1 + \eta_3) = \ln \frac{(\eta_1 + 2x_1)\left[2(1-x_1) + \eta_1\right]}{\left[2(1-x_1) - \eta_1\right](2x_1 - \eta_1)} ,$$

$$\frac{4w^{(1)}}{kT}\eta_3 - \frac{2w^{(2)}}{kT}(4\eta_3 + \eta_1 + \eta_5) = \ln \frac{(\eta_3 + 2x_3)\left[2(1-x_3) + \eta_3\right]}{\left[2(1-x_3) - \eta_3\right](2x_3 - \eta_3)} ,$$

. . .

and

$$\frac{8w^{(1)}}{kT}(x_1 + x_2 - x_1^b - 2x_2^b) + \frac{2w^{(2)}}{kT}(4x_1 + x_3 - 6x_1^b) - \frac{4}{kT}(U_{BB}^{(1)} - U_{AA}^{(1)} - w^{(1)})$$

$$- \frac{1}{kT}(U_{BB}^{(2)} - U_{AA}^{(2)} - w^{(2)}) = \ln \frac{\left[4(x_1^b)^2 - \eta_b^2\right]\left[4(1-x_1)^2 - \eta_1^2\right]}{\left[4(1-x_1^b)^2 - \eta_b^2\right](4x_1^2 - \eta_1^2)} ,$$

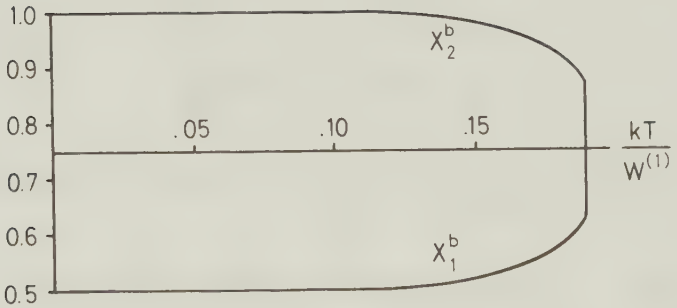

Fig. 31 Temperature dependence of the concentrations x_1^b and x_2^b referring to bulk (100) planes. $W^{(1)}$ is the energy of unmixing due to nearest neighbor bonds.

$$\frac{8W^{(1)}}{kT}(X_2 + X_1 + X_3 - X_1^b - 2X_2^b) + \frac{2W^{(2)}}{kT}(4X_2 + X_4 - 6X_1^b) - \frac{1}{kT}(U_{BB}^{(2)} - U_{AA}^{(2)} - W^{(2)})$$

$$= \ln \frac{[4(X_1^b)^2 - \eta_b^2](1-X_2)^2}{[4(1-X_1^b)^2 - \eta_b^2]X_2^2},$$

.
.
.

V.11

In the case where the surface plane is of type 2 the corresponding equations are

$$\frac{4W^{(1)}}{kT}\eta_2 - \frac{2W^{(2)}}{kT}(4\eta_2 + \eta_4) = \ln \frac{(\eta_2 + 2X_2)[2(1-X_2) + \eta_2]}{[2(1-X_2) - \eta_2](2X_2 - \eta_2)},$$

$$\frac{4W^{(1)}}{kT}\eta_4 - \frac{2W^{(2)}}{kT}(4\eta_4 + \eta_2 + \eta_6) = \ln \frac{(\eta_4 + 2X_4)[2(1-X_4) + \eta_4]}{[2(1-X_4) - \eta_4](2X_4 - \eta_4)},$$

.
.
.

V.12

and

$$\frac{8W^{(1)}}{kT}(X_1 + X_2 - X_1^b - 2X_2^b) + \frac{2W^{(2)}}{kT}(4X_1 + X_3 - 6X_1^b) - \frac{4}{kT}(U_{BB}^{(1)} - U_{AA}^{(1)} - W^{(1)})$$

$$- \frac{1}{kT}(U_{BB}^{(2)} - U_{AA}^{(2)} - W^{(2)}) = \ln \frac{[4(X_1^b)^2 - \eta_b^2](1-X_1)^2}{[4(1-X_1^b)^2 - \eta_b^2]X_1^2}$$

$$\frac{8W^{(1)}}{kT}\left(x_2+x_1+x_3-x_1^b-2x_2^b\right)+\frac{2W^{(2)}}{kT}\left(4x_2+x_4\right)-\frac{1}{kT}\left(U_{BB}^{(2)}-U_{AA}^{(2)}-W^{(2)}\right)$$

$$=\ln\frac{\left[4(x_1^b)^2-\eta_b^2\right]\left[4(1-x_2)^2-\eta_2^2\right]}{\left[4(1-x_1^b)^2-\eta_b^2\right]\left(4x_2^2-\eta_2^2\right)}\ ,$$

$$\vdots$$

V.13

In Fig. 32 we show for the bulk results for the order parameter $\eta_b(T)$ in order to illustrate the significance of taking into account next-nearest-neighbor bonds. Then using equations V.6 and V.7 we have calculated the temperature dependence of the order parameter in the vicinity of the (111) surface. In Fig. 33 we show results obtained for the (111) surface for η_1, η_2, η_3, etc., in the absence of surface segregation. In order to study the effect of surface segregation on atomic ordering, we show in Fig. 34(a) results for $\eta_i(T)$ obtained by taking into account the surface segregation shown in Fig. 34(b). Notice that both, surface segregation and atomic ordering have been calculated simultaneously from equations V.6 and V.7. In order to study how the atomic ordering depends on the surface geometry, results are shown in Fig. 35 and 36 for the order parameter in the surface layers for the case of a (100) surface. The results refer to the two different possible surface confi-

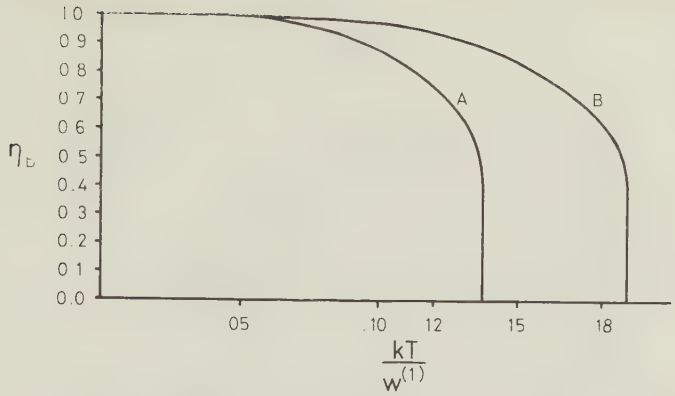

Fig. 32 Temperature dependence of the bulk order parameter. The curves A and B refer to $W^{(2)}=0$ and $W^{(2)}/W^{(1)}=.12$ respectively.

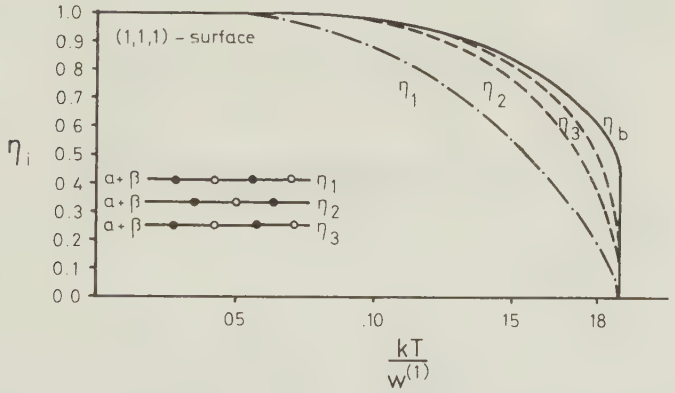

Fig. 33 Temperature dependence of the layer-dependent order parameters η_i for the (111) surface. Surface segregation is neglected. As indicated in the inlet figure each plane parallel to the surface consists of α- and β- sites. η_1, η_2, η_3 and η_b correspond to the first, second, third and bulk layer, respectively.

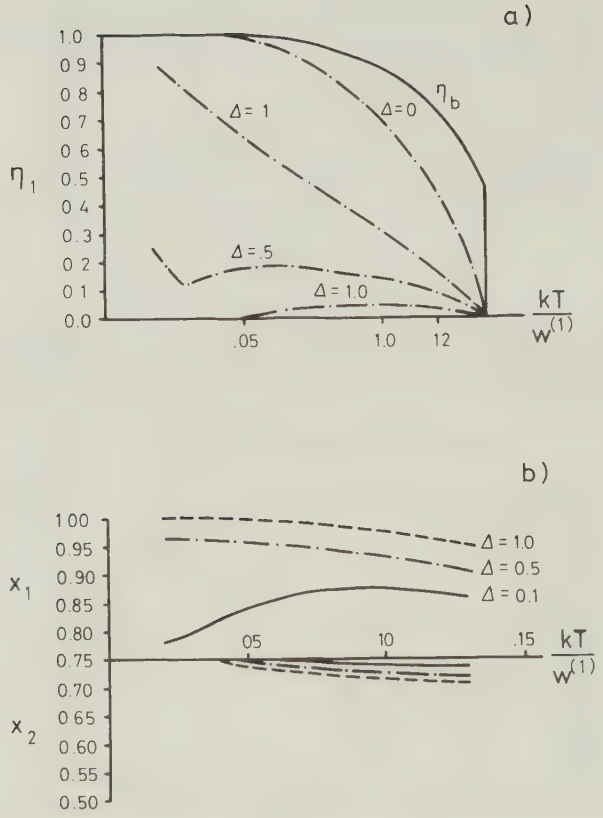

Fig. 34 a) Temperature dependence of the order parameter η_i at the (111) surface, taking into account the segregation shown in Fig.b) for different values $\Delta \equiv (U_{BB}^{(1)} - U_{AA}^{(1)})/W^{(1)}$. b) Results for the temperature dependence of surface segregation. The concentrations x_1 and x_2 refer to the first and second layer, respectively.

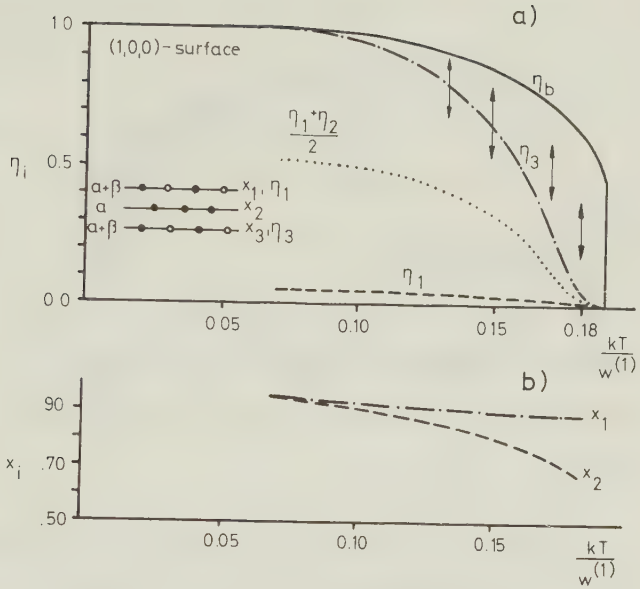

Fig. 35 a) Temperature dependence of the order parameters η_1, η_3 and $(\eta_1+\eta_3)/2$ at the (100) surface. The inlet figure shows schematically the surface configuration of Type 1 which has been used (see text). The bars represent experimental results[24]. b) Surface segregation vs. temperature.

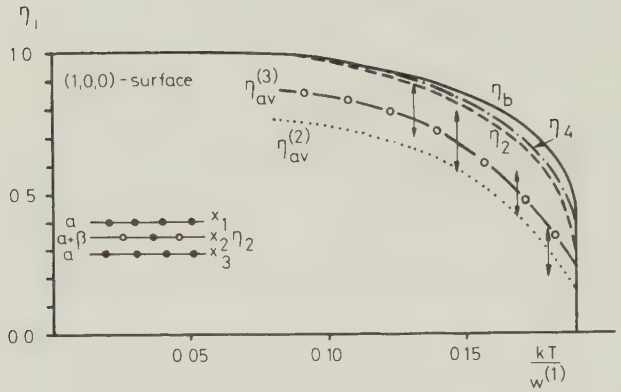

Fig. 36 Temperature dependence of the order parameters η_i at the (100) surface. As indicated in the inlet figure the surface configuration of type 2 has been assumed. Average order parameters $\eta_{ave}^{(2)} = \frac{1}{2}\{\frac{1}{2}(\eta_1+\eta_3)+\frac{1}{2}(\eta_2+\eta_4)\}$ and $\eta_{ave}^{(3)} = \frac{1}{2}\{\frac{1}{3}(\eta_1+\eta_3+\eta_5)+\frac{1}{3}(\eta_2+\eta_4+\eta_6)\}$ with respect to the two and three topmost $\alpha+\beta$ layers of the (100) surface configurations are shown by dots and circles, respectively. The experimental results[24] are shown by bars.

gurations.

In figure 36 the numerical results obtained for $\eta_i(T)$ using the Bragg-Williams approximation are compared with experimental results[24] obtained for Cu_3Au. Note that from the experiment one obtains an average order parameter. In the experiment one observes an order parameter which is averaged with respect to different possible atomic configurations at the (100) surface and which is also averaged over the surface region which is proved by the experiment. Therefore, the results shown in Fig. 36 for the average order parameters $\eta_{av}^{(2)} = \frac{1}{2}\left[\frac{1}{2}(\eta_1+\eta_3) + \frac{1}{2}(\eta_2+\eta_4)\right]$ and $\eta_{av}^{(3)} = \frac{1}{2}\left[\frac{1}{3}(\eta_1+\eta_3+\eta_5) + \frac{1}{3}(\eta_2+\eta_4+\eta_6)\right]$ should be compared with the experimental results. It is interesting that $\eta_{av}^{(3)}$ agrees better with the experiment than $\eta_{av}^{(2)}$. This might indicate that the LEED experiment[24] probes a surface area which corresponds more to the spatial average yielding $\eta_{av}^{(3)}$ than the one yielding $\eta_{av}^{(2)}$. As expected on physical grounds our numerical analysis yields that $\eta_{av}^{(2)}$ and $\eta_{av}^{(3)}$ increase for decreasing surface segregation. Therefore, the agreement with experimental results could be improved if values for the paremeter $(U_{AA}-U_{BB})$ are used which yield less segregation than was obtained in our calculation. Note the previous Monte Carlo calculations of $\eta_{av}^{(2)}$ assume no segregation. Also, it has been assumed in all our calculations that the bond energies do not change at the surface.

It is of interest to study the validity of this assumption within a microscopic electronic theory. Clearly, if the bond energies are concentration dependent, then the surface will cause them to change. Finally, note that for an irregular surface one has to average the order parameter over different surface configurations.

The theory presented could be easily extended by determining U within a microscopic electronic theory, for example, by using $U = \sum_i U_i$ and $U_i = \int dE E N_i(E)$, where $N_i(E)$ is the electronic density of states referring to the i-th layer parallel to the surface. However, as long as the energies of unmixing $W^{(1)}$ and $W^{(2)}$ are only weakly concentration dependent, the Bragg-Williams approximation should be sufficient.

We find that only the η_i for the first few atomic surface layers are strongly reduced. Comparing the results for η_i obtained at the (111) surface, see Figs. 32 and 33 with those at the (100) surface, see Figs. 34 and 35, one notes that the reduction of $\eta_i(T)$ depends strongly on the surface geometry. The results shown in Figs. 33 and 34 indicate that surface segregation may have a strong effect on atomic ordering. Note that at T_C all η_i desappear. In view of the fact that approximately $T_C \propto x(1-x)$, one might expect due to surface segregation ($x_i \neq x_b$) that at the surface $T_C \lesseqgtr T_C^{bulk}$ depending on $x \gtrless 0.5$. However, if the surfa-

ce segregation occurs over a distance d away from the surface, then for $d<\xi_\perp(T)$ all $\eta_i(T)$ disappear at the same temperature and hence $T_C^{surface}=T_C^{bulk}$. $\xi_\perp(T)$ refers to the correlation length measuring atomic ordering in a direction perpendicular to the surface. However, note that for $d> \xi_\perp(T)$ it seem possible that $T_C^{surface}\neq T_C^{bulk}$. This argument explains why due to surface segregation $\eta_i(T)\to 0$ $i=1,2$ at temperatures below T_C, where $\xi_\perp(T)\to 0$ (see the results shown in Fig. 33).

More local experiments would be desirable for a comparison with our numerical results for $\eta_1(T)$, $\eta_2(T)$, etc., obtained for different surface geometries. In particular, it would be interesting to check experimentally our results (see Fig. 33) obtained in the presence of segregation. It would be interesting to study order-disorder transitions in alloys A_xB_{1-x} with $x_b<0.5$ and surface segregation such that at the surface $x>x_b$.

In the disordered case, the equations that determine the concentrations x_i reduce to the equations for segregation in regular solutions[57,59]. Here we have assumed no surface relaxation, but since the effect of relaxation is to reduce the segregation, if the pair bonds at the surface are stronger[57], we expect a less drastic reduction for the surface order parameters in that case.

Our results shown in Fig. 33 indicate that surface

segregation and atomic ordering affect each other. We find that for A_3B-type alloys segregation always tries to destroy the atomic order, but also the ordering can suppress segregation if the difference $\Delta=(U_{AA}^{(1)}-U_{BB}^{(1)})/W^{(1)}$ is small. Until now theories that describe surface enrichment in ordered alloys have assumed the same order at the surface and in bulk[72,73].

Note, if $x_i^s \; x_b$ and if $T_c(x)$ increases for increasing x, then $n_i^s(T)>n_b(T)$ at $T<T_c$ may be possible.

It is of considerable interest to study the effect of the surface on the order-disorder transition by using a microscopic theory for the electronic structure at the surface. Thus, the dependence of order-disorder phenomena at the surface on the various electronic parameters, electron charge transfer, chemisorbed atoms and molecules, etc. may be studied. In Appendix D we present such a microscopic theory for surface effects on order-disorder phenomena.

VI. CONCLUSIONS

We have presented a microscopic theory for the electronic structure at transition metal alloy surfaces, which play an important role in catalysis. Our theory is relatively simple and needs to be improved, for example, in order to study in detail the electronic density of states at the surface of alloys and important effects due to the interplay of the s-electron and d-electron charge redistribution at the surface. Nevertheless our results are instructive for what one may expect in a more realistic theory and demostrates the significance of various electronic parameters for chemisorption, segregation, selectivity, order disorder phase transitions, etc..

Due to the various approximations used in the theory presented here our results should apply best to CuNi and similar alloys. Due to the approximation $\Delta_\ell^{ij} = \Delta_\ell^j$ and the neglection of terms of higher order than t^2 in Δ_i and Δ_ℓ^j, etc., we obtain simplified local density of states $N_i(E)$ without fine structure. Consequently, we have to extend our theory in order to determine surface properties which depend on the detailed structure present in $N_i(E)$. However, the good agreement between the results obtained for the bulk $N_i(E)$ with our theory and the coherent potential

approximation suggest that our theory should give correctly the overall shape of the local density of states. Furthermore, the good agreement of our results obtained for the local density of states of an atoms chemisorbed on a substrate of the same kind and those obtained by Cyrot-Lackmann et al.[9] using the moment expansion technique indicates that the approximations used in this paper do not restrict too much the validity of the results obtained for the local density of states and therefore, the results for the binding energy, surface segregation, order-disorder phase transition, etc.

In this work we have presented, in contrast to previous phenomenological theories, a microscopic theory for the electronic forces responsible for surface segregation in transition metal alloys. This theory is not restricted to rigid-band-type alloys, and in contrast to Bragg-Williams type theories it is also valid if $\Delta U/x(1-x)=2U_{AB}-U_{AA}-U_{BB}$ is a function of x, as will be the case for many alloys. Also, this theory permits a systematic study of the important electronic parameters which determine surface segregation in d-band metals. This theory can also be applied to study solubility profiles at surface and melting at the surface.

We find that surface segregation occurs essentially only within the first three atomic layers at the surface

that it depends sensitively on the d-band filling, e.g., on the difference $n_A - n_B$, and on the difference $\delta = \varepsilon_A - \varepsilon_B$, that it weakens with increasing temperature, and that it depends strongly on the alloy composition as seen by the crossover curves $x_i = x_i(x_b)$. Also it affects the alloy solubility range. Here, we have studied only alloys with mixing energies $\Delta U = 2U_{AB} - U_{AA} - U_{BB} > 0$. The application of our theory for alloys with $\Delta U < 0$ (tendency to order) is straightforward. We have also neglected the posibility of concentration fluctuations within the planes parallel to the surface. These fluctuations corresponding to the existence of short range order are important for magnetism, selectivity, etc., and a detailed study of this problem would be of relevance.

We have shown that in order to explain the selective catalytic behaviour of transition metal alloy catalysts local environment effects and surface segregation have to be taken into account. In our calculation for the binding enrgy we have used a simple model adatom to describe reactions of C-atoms. It seems reasonable to assume that the binding energy for a more realistic description of the C-atoms will exhibit the same evironmental dependence as obtained in our model calculation.

We have also presented a Bragg-Williams-type theory and a simple electronic theory for the effect of the surface on the order-disorder phenomena. We find that within

the first atomic layers at the surface the atomic ordering is strongly reduced due to the surface. In view of the fact that approximately $T_C \propto x(1-x)$ one might expect that due to segregation ($x_i \neq x_b$) that at the surface $T_C^s \gtrless T_C^{bulk}$ depending on $x \gtrless 0.5$. However, if the surface segregation occurs over a distance d away from the surface then for $d < \xi_\perp(T)$ all $\eta_i(T)$ disapper at the same temperature and hence $T_C^s = T_C^{bulk}$. $\xi_\perp(T)$ refers to the correlation lenght measuring atomic ordering in a direction perpendicular to the surface. Here we have found that T_C is the same for all layers. We showed that the effect of the surface on the order-disorder phase transition is different for differnt surface geometry, and that surface segregation has a strong effect on atomic ordering as well as atomic ordering can suppress surface segregation.

The theory developed here can be used to study several other problems in surface physics. The coverage dependence on the change in work function due to chemisorption, the coverage dependence of the binding energy of chemisorbed atoms, the effect of order-disorder transitions in chemisorbed layers on the work function, the influence of surface irregularities, like steps, knicks or holes, on the surface properties, etc., are some examples.

APPENDIX A. DETERMINATION OF G_{ii} IN THE PRESENCE OF s-d HYBRIDIZATION

In order to treat the coupling between s and d-electrons near the surface we use the model Hamiltonian given by the equation II.1 and add to it the terms[49]

$$\sum_{k\sigma} \varepsilon_k c^{\dagger}_{k\sigma} c_{\sigma}$$

and

$$H_{s-d} = \sum_{n,k} \gamma_n c^{\dagger}_{k\sigma} c_{n\sigma} e^{i\vec{k}\cdot\vec{R}_n} + h.c. \qquad A.1$$

Here, ε_k denotes the enrgy of an s-electron with wave-vector k and $c^{\dagger}_{k\sigma}$ and $c_{k\sigma}$ are the usual creation and annihilation operators for s-electrons with spin σ. The term H_{s-d} describes electronic transitions between s- and d-states and γ_n is the hybridization constant[49] on site n. Then because of the term H_{s-d} in the Hamiltonian the theory described in Chapter II A) gets modified as follows. It is now

$$G_{ii}(E) = (E - \varepsilon_i - \gamma^2 G_s - \Delta_i)^{-1} \qquad A.2$$

with

$$\Delta_i = \sum_{j \neq i} \frac{t_{ij} t_{ji}}{E - \varepsilon_j - \gamma_j^2 G_s - \Delta_j^i} + \ldots \qquad \text{A.3}$$

where

$$\Delta_j^i = \sum_{\ell \neq i,j} \frac{t_{j\ell} t_{\ell j}}{E - \varepsilon_\ell - \gamma_\ell^2 G_s - \Delta_\ell^{ij}} + \ldots \qquad \text{A.4}$$

and where $G_s(E) = \sum_k (1/(E-\varepsilon_k))$. It follows that equations II.11 to II.18 still hold if we replace ε_j by $\varepsilon_j + \gamma_j^2 G_s$. Notice that the coherent potential approximation type theory outlined in Appendix B can be similarly modified to include s-d hybridization.

APPENDIX B. COHERENT POTENTIAL APPROXIMATION AND ITS EXTENSION THE BETHE-PEIERLS APPROXIMATION FOR AN ALLOY SURFACE

In the following the Bethe-Peierls approximation extension of the coherent potential approximation is used to determine $G_{ii}=(E-\varepsilon_i-\Delta_i)^{-1}$, with Δ_i given by equation II.4. Using for Δ_j^i the approximation $\Delta_b^{II}=\Delta$, $\Delta_I^{II}=\Delta_I^I$, $\Delta_{II}^I=\Delta_{II}^{II}$ the Δ_I^I and Δ_{II}^{II} are approximately determined by

$$\Delta_I = \frac{z_1 t^2}{E - \Sigma_I - \Delta_I^I} + \frac{z_0 t^2}{E - \Sigma_{II} - \Delta_{II}^{II}} \qquad \text{B.1}$$

and

$$\Delta_{II} = \frac{z_0 t^2}{E - \Sigma_{II} - \Delta_{II}^{II}} + \frac{z_1 t^2}{E - \Sigma_I - \Delta_I^I} + \frac{z_1 t^2}{E - \Sigma - \Delta} \qquad \text{B.2}$$

with

$\Delta_I=E-\Sigma_I-F_I^{-1}$, $\Delta_{II}=E-\Sigma_{II}-F_{II}^{-1}$ and $\Delta=E-\Sigma-F^{-1}$.

The average electron energy within the first layer and second layer is denoted by Σ_I and Σ_{II}, respectively. Σ refers to the bulk metal. F_I denotes in the Wannier re-

presentation, the Green's function for an electron on a site belonging to the first atomic layer and is determined for a metal in which the atomic energy levels $\varepsilon_{I,A}$, $\varepsilon_{I,B}$, $\varepsilon_{II,A}$, $\varepsilon_{II,B}$ and ε_A, ε_B are replaced by Σ_I, Σ_{II} and Σ respectively. Similarly, F_{II} and F which refer to the second layer and the bulk metal respectively are determined. The electron self energies Σ_I, Σ_{II} and Σ are approximately determined by

$$F_I = xG_{I,A} + (1-x)G_{I,B} \qquad B.3$$

$$F_{II} = xG_{II,A} + (1-x)G_{II,B} \qquad B.4$$

and

$$F = xG_A + (1-x)G_B \qquad B.5$$

Note that using equations B.1 and B.2 one can readily express Δ_I^I and Δ_{II}^{II} in terms of Δ_I, Δ_{II}, Δ, Σ_I, Σ_{II}, z_0 and z_1 by

$$\Delta_I^I = E-\Sigma_I-(z_1^2-z_0^2)t^2\{z_1(E-\Sigma_{II}-F_{II}^{-1})-z_0(E-\Sigma_I-F_I^{-1}) + z_1z_0t^2(E-\Sigma-\Delta)^{-1}\}^{-1}$$

and

$$\Delta_{II}^{II} = E-\Sigma_{II}-(z_1^2-z_0^2)t^2\{z_1(E-\Sigma_I-F_I^{-1})-z_0(E-\Sigma_{II}-F_{II}^{-1}) + z_1z_0t^2(E-\Sigma-\Delta)^{-1}\}^{-1}$$

Then, these expressions for Δ_I^I and Δ_{II}^{II} resulting from equations B.1 and B.2 are used in equation B.3 to determine Δ_I and Δ_{II} and consequently $G_{I,i}$ and $G_{II,i}$.

APPENDIX C. DETERMINATION OF THE INTERNAL ENERGY U AS A FUNCTION OF THE ORDER PARAMETERS

The internal energy is given by

$$U = \sum_{i=1}^{N} (U_i^{(1)} + U_i^{(2)}),$$

where

$$U_i^{(n)} = -\frac{2}{z_n}\left[N_{AA}^{i,i(n)} U_{AA}^{i,i(n)} + \frac{1}{2}\left(N_{AA}^{i,i\pm1(n)} U_{AA}^{i,i\pm1(n)} \right) + N_{BB}^{i,i(n)} U_{BB}^{i,i(n)} \right.$$

$$\left. + \frac{1}{2}\left(N_{BB}^{i,i\pm1(n)} U_{BB}^{i,i\pm1(n)} \right) + N_{AB}^{i,i(n)} U_{AB}^{i,i(n)} + \frac{1}{2}\left(N_{AB}^{i,i\pm1(n)} U_{AB}^{i,i\pm1} \right) \right]$$

Here, z_1 and z_2 are the number of nearest and next-nearest-neighbors, $N_{AA}^{i,i(n)}$ are the number of A-A nearest (n=1) and next-nearest-neighbor (n=2) atomic pairs in the i-th layer with $U_{AA}^{i,i(n)}$ bond energies. All the other quantities have a similar meaning.

Using Table 1 and the probabilities given by equation IV.5 we get for the (111) surface the expressions

$$N_{AA}^{1,1(1)} = \frac{3}{2} N_{11}\left[(x_1 - \frac{3}{4}\eta_1)(x_1 + \frac{1}{4}\eta_1) + (x_1 + \frac{1}{4}\eta_1)^2 \right],$$

$$N_{AA}^{1,2(1)} + N_{AA}^{2,1(1)} = \frac{3}{4} N_{11}\left\{ (x_1 - \frac{3}{4}\eta_1)(x_2 + \frac{1}{4}\eta_2) \right.$$

$$\left. + (x_1 + \frac{1}{4}\eta_1)\left[2(x_2 + \frac{1}{4}\eta_2) + (x_2 - \frac{3}{4}\eta_2) \right] \right\},$$

$$\vdots$$

$$N_{BB}^{1,1(1)} = \frac{3}{2} N_{II}\left[(1-x_1+\frac{3}{4}\eta_1)(1-x_1-\frac{1}{4}\eta_1) + (1-x_1-\frac{1}{4}\eta_1)^2\right],$$

$$N_{BB}^{1,2(1)} + N_{BB}^{2,1(1)} = \frac{3}{4} N_{II}\Big\{(1-x_1+\frac{3}{4}\eta_1)(1-x_2-\frac{1}{4}\eta_2)$$

$$+ (1-x_1-\frac{1}{4}\eta_1)\left[2(1-x_2-\frac{1}{4}\eta_2) + (1-x_2+\frac{3}{4}\eta_2)\right]\Big\},$$

$$\vdots$$

$$N_{AB}^{1,1(1)} = 3N_{II} - N_{AA}^{1,1(1)} - N_{BB}^{1,1(1)},$$

$$N_{AB}^{1,2(1)} + N_{AB}^{2,1(1)} = \frac{3}{2} N_{II} - \left(N_{AA}^{1,2(1)} + N_{AA}^{2,1(1)}\right) - \left(N_{BB}^{1,2(1)} + N_{BB}^{2,1(1)}\right),$$

$$\vdots$$

and for next-nearest-neighbor atomic pairs

$$N_{AA}^{1,1(2)} = 0,$$

$$N_{AA}^{1,2(2)} + N_{AA}^{2,1(2)} = \frac{3}{4} N_{II}\left[(x_1-\frac{3}{4}\eta_1)(x_2-\frac{3}{4}\eta_2) + 3(x_1+\frac{1}{4}\eta_1)(x_2+\frac{1}{4}\eta_2)\right],$$

$$\vdots$$

$$N_{BB}^{1,1(2)} = 0,$$

$$N_{BB}^{1,2(2)} + N_{BB}^{2,1(2)} = \frac{3}{4} N_{II}\left[(1-x_1+\frac{3}{4}\eta_1)(1-x_2+\frac{3}{4}\eta_2) + 3(1-x_1-\frac{1}{4}\eta_1)(1-x_2-\frac{1}{4}\eta_2)\right]$$

$$\vdots$$

$$N_{AB}^{1,1(2)} = 0,$$

$$N_{AB}^{1,2(2)} + N_{AB}^{2,1(2)} = \frac{3}{2} N_{II} - \left(N_{AA}^{1,2(2)} + N_{AA}^{2,1(2)}\right) - \left(N_{BB}^{1,2(2)} + N_{BB}^{2,1(2)}\right),$$

$$\vdots$$

Site in the i-th layer	a)	b)	c)	d)	e)	f)	g)	h)
α	4	2	2	1	0	0	3	0
β	6	0	3	0	0	0	0	3

TABLE 1: Number of nearest- and next-nearest-neighbors for each α- and β-site in the (111)planes.

a) Number of nearest-neighbor α-sites in the i-th layer.

b) Number of nearest-neighbor β-sites in the i-th layer.

c) Number of nearest-neighbor α-sites in the i±1-th layer.

d) Number of nearest-neighbor β-sites in the i±1-th layer.

e) Number of next-nearest-neighbor α-sites in the i-th layer.

f) Number of next-nearest-neighbor β-sites in the i-th layer.

g) Number of next-nearest-neighbor α-sites in the i±1-th layer.

h) Number of next-nearest-neighbor β-sites in the i±1-th layer.

Site in the i-th layer	a)	b)	c)	d)	e)	f)	g)	h)
α Type 1	0	4	4	0	4	0	1	0
α Type 2	4	0	2	2	4	0	1	0
β	4	0	4	0	0	4	0	1

TABLE 2: Number of nearest- and next-nearest-neighbors for each α- and β-site in the two types of (100) planes.

The columns a), b), c), d), e) and f) have the same meaning as in Table 1.

g) Number of next-nearest-neighbor α-sites in the i±2-th layer.

h) Number of next-nearest-neighbor β-sites in the i±2-th layer.

In the (100) surface we obtain using Table 2 and the equations IV.9 for the surface configuration type 1 the expressions

$$N_{AA}^{1,1(1)} = 2N_{II}\left(x_1 - \tfrac{1}{2}\eta_1\right)\left(x_1 + \tfrac{1}{2}\eta_1\right),$$

$$N_{AA}^{1,2(1)} + N_{AA}^{2,1(1)} = 4N_{II}x_1x_2,$$

$$\vdots$$

$$N_{BB}^{1,1(1)} = 2N_{II}\left(1 - x_1 - \tfrac{1}{2}\eta_1\right)\left(1 - x_1 + \tfrac{1}{2}\eta_1\right),$$

$$N_{BB}^{1,2(1)} + N_{BB}^{2,1(1)} = 4N_{II}(1 - x_1)(1 - x_2),$$

$$\vdots$$

$$N_{AB}^{1,1(1)} = 2N_{II} - N_{AA}^{1,1(1)} - N_{BB}^{1,1(1)}$$

$$N_{AB}^{1,2(1)} + N_{AB}^{2,1(1)} = 2N_{II} - \left(N_{AA}^{1,2(1)} + N_{AA}^{2,1(1)}\right) - \left(N_{BB}^{1,2(1)} + N_{BB}^{2,1(1)}\right)$$

$$\vdots$$

and for next-nearest-neighbor atomic pairs

$$N_{AA}^{1,1(2)} = N_{11}\left[\left(x_1+\tfrac{1}{2}\eta_1\right)^2+\left(x_1-\tfrac{1}{2}\eta_1\right)^2\right],$$

$$N_{AA}^{1,3(2)} + N_{AA}^{3,1(2)} = \frac{N_{11}}{2}\left[\left(x_1+\tfrac{1}{2}\eta_1\right)\left(x_3+\tfrac{1}{2}\eta_3\right)+\left(x_1-\tfrac{1}{2}\eta_1\right)\left(x_3-\tfrac{1}{2}\eta_3\right)\right],$$

$$\vdots$$

$$N_{BB}^{1,1(2)} =$$

$$N_{BB}^{1,3(2)} + N_{BB}^{3,1(2)} = \frac{N_{11}}{2}\left[\left(1-x_1+\tfrac{1}{2}\eta_1\right)\left(1-x_3+\tfrac{1}{2}\eta_3\right)\right.$$

$$\left.+\left(1-x_1-\tfrac{1}{2}\eta_1\right)\left(1-x_3-\tfrac{1}{2}\eta_3\right)\right]$$

$$\vdots$$

$$N_{AB}^{1,1(2)} = 2N_{11} - N_{AA}^{1,1(2)} - N_{BB}^{1,1(2)}$$

$$N_{AB}^{1,3(2)} + N_{AB}^{3,1(2)} = \frac{N_{11}}{2} - \left(N_{AA}^{1,3(2)} + N_{AA}^{3,1(2)}\right) - \left(N_{BB}^{1,3(2)} + N_{BB}^{3,1(2)}\right)$$

$$\vdots$$

It is easy to derive for the surface configuration of Type 2 a similar set of expressions.

APPENDIX D. ELECTRONIC THEORY FOR THE ORDER-DISORDER TRANSITION AT THE SURFACE OF BINARY ALLOYS

Recently, several authors have described the order-disorder phase transition in the bulk medium using a band model calculation. All these calculations have been done in the coherent potential approximation (CPA)[74-77].

Here we present such a calculation for the order-disorder transition at the surface. A continued fraction technique is used for determining the local electronic Green's functions on the surface of a semi-infinite crystal. We assume that only the first three layers near the surface are affected by the surface. We find that atomic ordering occurs at T_C in the bulk as well as at the surface.

Consider a binary alloy A_xB_{1-x} with N lattice points and assume that these lattice points can be subdivided into two sublattices α and β, such that there are $\frac{1}{2}N$ sites of type α and $\frac{1}{2}N$ sites of type β. Each α-site has z β-sites as its nearest neighbors and each β-site has z α-sites as its nearest neighbors. We consider the simple case of a simple cubic lattice and an alloy with concentration 0.5. If the number of A-atoms on the α-sites is denoted by $\frac{1}{2}(1+\eta)\frac{1}{2}N$, then the order parameter η varies between 0 and 1. Since all atoms which are not in α-sites are in β-sites and all sites are occupied by A- or B-atoms, we have the following

distribution:

$$N_{\alpha}^{A} = \frac{1}{2}(1+\eta)\frac{1}{2}N = N_{\beta}^{B}$$
$$N_{\beta}^{A} = \frac{1}{2}(1-\eta)\frac{1}{2}N = N_{\alpha}^{B} \qquad \text{D.1}$$

If $\eta=1$ (the complete order case) all the A-atoms are in the α-sublattice and all B-atoms are in the β-sublattice. If $\eta=0$ (the complete disordered case), there are as many A-toms on α-sites as on β-sites and the same holds for B-atoms. Values of η between 0 and 1 correspond to intermediate degrees of order.

The electrons in the binarry alloy are described by the tight-binding Hamiltonian

$$H = \sum_{\alpha} \varepsilon_{\alpha} c_{\alpha}^{\dagger} c_{\alpha} + \sum_{\beta} \varepsilon_{\beta} c_{\beta}^{\dagger} c_{\beta} + \sum_{\alpha \neq \beta} t c_{\alpha}^{\dagger} c_{\beta} \qquad \text{D.2}$$

Here, the electronic energy levels of atoms sitting in the α- and β-sublattices take the values ε_A and ε_B with probabilities

$$p_{\alpha}^{A} = \frac{1}{2}(1+\eta), \qquad p_{\beta}^{B} = \frac{1}{2}(1-\eta)$$

and $\qquad \text{D.3}$

$$p_{\beta}^{A} = \frac{1}{2}(1-\eta), \qquad p_{\alpha}^{B} = \frac{1}{2}(1+\eta)$$

respectively. $c_{\alpha}^{\dagger}$, $c_{\beta}^{\dagger}$, c_{α}, c_{β} are the usual electronic

creation and annihilation operators referring to sites in the α- and β-sublattices. The hopping integral t describes electronic transitions between sites in the α- and β-sublattices. The average local electronic Green's function $G_{\alpha\alpha}$ on sites in the α-sublattice is given by

$$G_{\alpha\alpha}(E,n) = \frac{p_\alpha^A}{E-\varepsilon_A-\Delta_\alpha} + \frac{p_\beta^B}{E-\varepsilon_B-\Delta_\alpha} \qquad \text{D.4}$$

Here, Δ_α is the electron self-energy resulting from the electron hopping processes starting and ending at the site i of the α-sublattice

$$\Delta_\alpha = \sum_\beta \frac{t_{\alpha\beta}t_{\beta\alpha}}{E-\varepsilon_\beta-\Delta_\beta^\alpha} + \ldots\ldots$$

$$= zt^2\left(\frac{p_\beta^A}{E-\varepsilon_A-\Delta_\beta^\alpha} + \frac{p_\beta^B}{E-\varepsilon_B-\Delta_\beta^\alpha}\right) + \ldots \qquad \text{D.5}$$

In a similar way one finds approximately

$$\Delta_\beta^\alpha = (z-1)t^2\left(\frac{p_\alpha^A}{E-\varepsilon_A-\Delta_\alpha^\beta} + \frac{p_\alpha^B}{E-\varepsilon_B-\Delta_\alpha^\beta}\right). \qquad \text{D.6}$$

The continued fraction is approximated by

$$\Delta_\alpha^\beta = (z-1)t^2\left(\frac{p_\beta^A}{E-\varepsilon_A-\Delta_\beta^\alpha} + \frac{p_\beta^B}{E-\varepsilon_B-\Delta_\beta^\alpha}\right). \qquad \text{D.7}$$

Thus, we get for Δ_β^α the equation

$$\Delta_\beta^\alpha = (z-1)t^2\left(\frac{p_\alpha^A}{E-\epsilon_A-(z-1)t^2\left(\frac{p_\beta^A}{E-\epsilon_A-\Delta_\beta^\alpha}+\frac{p_\beta^B}{E-\epsilon_B-\Delta_\beta^\alpha}\right)} + \frac{p_\alpha^B}{E-\epsilon_B-(z-1)t^2\left(\frac{p_\beta^A}{E-\epsilon_A-\Delta_\beta^\alpha}+\frac{p_\beta^B}{E-\epsilon_B-\Delta_\beta^\alpha}\right)} \right). \qquad \text{D.8}$$

This equation can be rewritten as a fifth order equation in Δ_β^α as a function of z, ϵ_A, ϵ_B, η and E.

The average local Green's function for the β-sublattice is given by

$$G_{\beta\beta}(E,\eta) = \frac{p_\beta^A}{E-\epsilon_A-\Delta_\beta} + \frac{p_\beta^B}{E-\epsilon_B-\Delta_\beta}\ , \qquad \text{D.9}$$

with

$$\Delta_\beta = zt^2\left(\frac{p_\alpha^A}{E-\epsilon_A-\Delta_\alpha^\beta}+\frac{p_\alpha^B}{E-\epsilon_B-\Delta_\alpha^\beta}\right). \qquad \text{D.10}$$

Then, the average local density of states is calculated from

$$N(E,\eta) = -\frac{1}{2\pi}\,\mathrm{Im}\{\,G_{\alpha\alpha}(E,\eta) + G_{\beta\beta}(E,\eta)\} \qquad \text{D.11}$$

To calculate the order parameter η we minimize the free energy

$$F(n) = U(n) - TS(n) \qquad D.12$$

with respect to n. Here, the internal energy is given by

$$U(n) = \int_{-\infty}^{E_F} dE\ EN(E,n) \qquad D.13$$

and the entropy is given by $S(n)=S_0+\Delta S(n)$,

$$\Delta S = -k\ (\frac{1+n}{2}\ln\frac{1+n}{2} + \frac{1-n}{2}\ln\frac{1-n}{2}). \qquad D.14$$

In order to apply this theory for studing surface effects, we assume that the surface affects only the first three layers near the surface. We introduce then as before layer dependent long-range order paremeters n_i, which describe the atomic order in the i-th layer parallel to the surface.

The local Green's function depends then also on a layer index

$$G^i_{\alpha\alpha}(E) = \frac{p_A^{\alpha i}}{E-\varepsilon_{A,i}-\Delta_\alpha^i} + \frac{p_B^{\alpha i}}{E-\varepsilon_{B,i}-\Delta_\alpha^i},$$

where

$$\Delta_\alpha^i = z_0 t_{ii}^2 (\frac{p_A^{\beta i}}{E-\varepsilon_{A,i}-\Delta_{\beta i}^{\alpha i}} + \frac{p_B^{\beta i}}{E-\varepsilon_{B,i}-\Delta_{\beta i}^{\alpha i}}) + z_1 \sum_{j=i\pm1} t_{ij}^2 (\frac{p_A^{\beta j}}{E-\varepsilon_{A,j}-\Delta_{\beta j}^{\alpha i}} + \frac{p_B^{\beta j}}{E-\varepsilon_{A,j}-\Delta_{\beta j}^{\alpha i}}) \qquad D.15$$

Here, $p_A^{\alpha i}$ and $p_B^{\alpha i}$ are the probabilities to find an A- or B-atom in the i-th layer in the α-sublattice, and are given by

$$p_A^{\alpha i} = \frac{1}{2}(1+\eta_i), \qquad p_B^{\alpha i} = \frac{1}{2}(1-\eta_i) \qquad \text{D.16}$$

t_{ii} is the hopping integral between atoms in the same layer and $t_{ii\pm1}$ is the hopping integral between atoms in the i-th and the i±1-th layers. z_0 is the number of nearest-neighbors laying in the i-th layer and z_1 is the number of nearest-neighbors in the adyacent layer. $\Delta_{\beta i}^{\alpha i}$ refers to the self-energy which results from electron hopping processes starting and ending in a site in the i-th layer of the β-sublattice and avoiding a site in the same layer of the α-sublattice.

Using the same technique as before, see equation D.8, one obtains

$$\Delta_{\beta i}^{\alpha i} = (z_0 - 1)\, t^2 \left[\frac{\frac{1}{2}(1+\eta_i)}{E - \epsilon_{A,i} - \Delta_{\alpha i}^{\beta i}} + \frac{\frac{1}{2}(1-\eta_i)}{E - \epsilon_{B,i} - \Delta_{\alpha i}^{\beta i}} \right]$$

$$+ z_1 \sum_{j=i\pm1} t_{ij}^2 \left[\frac{\frac{1}{2}(1+\eta_j)}{E - \epsilon_{A,j} - \Delta_{\alpha j}^{\beta i}} + \frac{\frac{1}{2}(1-\eta_j)}{E - \epsilon_{B,j} - \Delta_{\alpha j}^{\beta i}} \right]$$

$$\vdots \qquad \text{D.17}$$

We may proceed by writing

$$U = \sum_i U_i \qquad D.18$$

where U_i is given by the expression

$$U = \int_{-\infty}^{\epsilon_F} dE\ EN_i(E,\ldots,\eta_{i-1},\eta_i,\eta_{i+1},\ldots) \qquad D.19$$

and where the electronic density of states $N_i(E,\ldots\eta_{i-1},\eta_i\cdot)$ referring to the i-th layer is given by

$$N_i(E..,\eta_i,\ldots) = -\frac{1}{2}\{\mathrm{Im}\ G^i_{\alpha\alpha}(E..,\eta_i,..)+G^i_{\beta\beta}(E..,\eta_i,..)\} \qquad D.20$$

Note, the energy U_i depends now approximately only on η_{i-1}, η_i and η_{i+1}. As before, the entropy is written in the form

$$\Delta S = \sum_i \Delta S_i,$$

where

$$\Delta S_i = -k\left(\frac{1+\eta_i}{2}\ln\frac{1+\eta_i}{2} + \frac{1-\eta_i}{2}\ln\frac{1-\eta_i}{2}\right).$$

In order to compare our simple theory with more elaborated theories[76,77] we show in Fig. 37 results for the bulk local density of states as a function of the energy and the long range order. Note, these results are in fair ageement with those shown by Plishke and Mattis[76] using a generalized form of the coherent potential approximation. In Fig. 38 the results are shown for the order parameter $\eta_i(T)$. We see

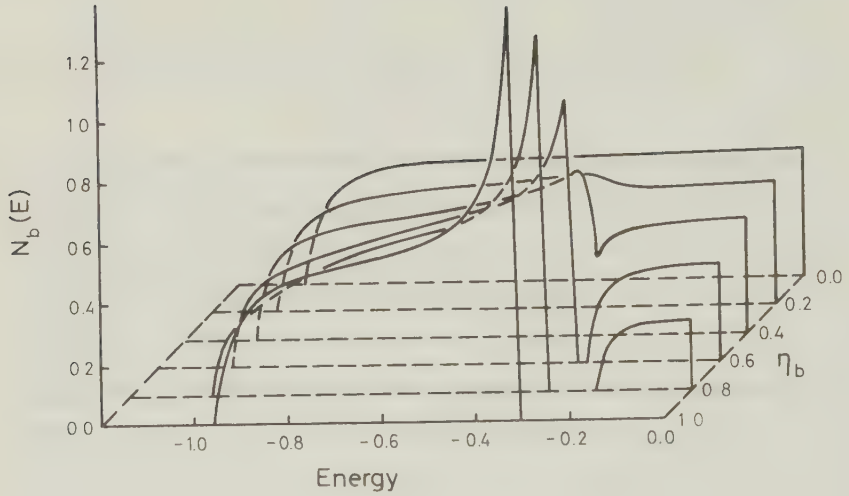

Fig. 37 Bulk local density of states $N_b(E)$ for $\delta=\varepsilon_A-\varepsilon_B=0.6$ and for several values of η_b. We show only the lower-half of the band since $N_b(E)$ is symmetric.

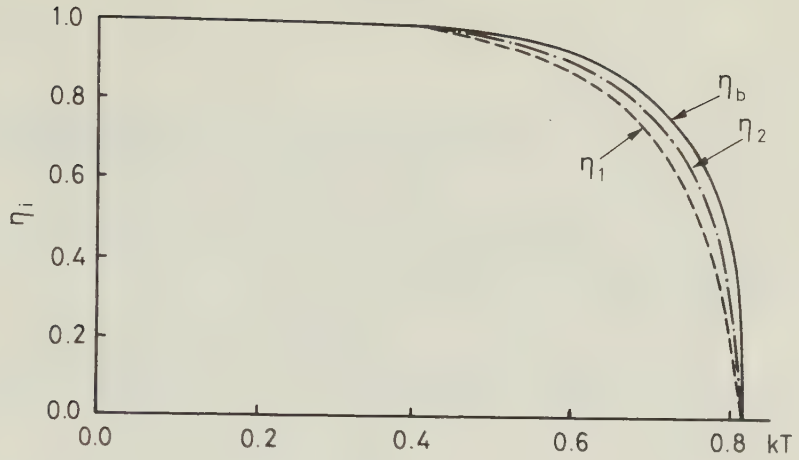

Fig. 38 Temperature dependence of the order parameters η_1, η_2 and η_b using δ=0.6 and for the hopping integral $t_{surf}=t_{bulk}$.

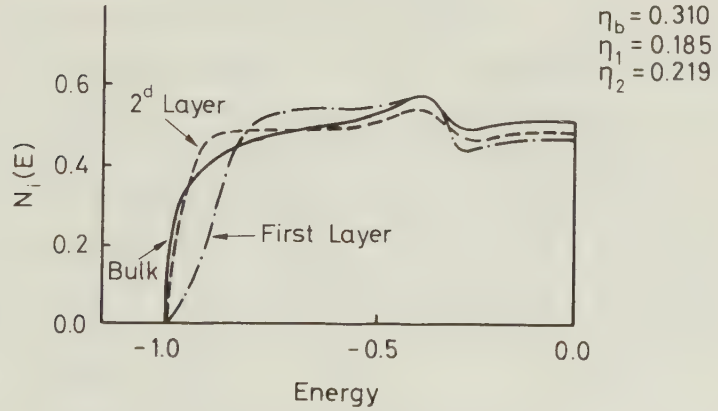

Fig. 39 Layer-dependent local density of states $N_1(E)$, $N_2(E)$ and $N_b(E)$ referring to the first-, second- and bulk layer for the indicated set of η_1, η_2,...η_b equilibrium values.

that the effect of the surface is not strong. However, this is only so because for a simple cubic lattice the coordination number is reduced only by one at the (100) surface. Also results for the average local density of states in the first two layers are shown in Fig. 35.

It is of interest to expand the internal energy U_i and S_i near T_C as a function of the order parameters. One then obtains for the free energy the expression

$$F_i(E,..\eta_{i-1},\eta_i,\eta_{i+1},..) = F_i^0 + \frac{\partial F}{\partial \eta_i}\eta_i + \sum_{j=i\pm1} \frac{\partial F}{\partial \eta_j}\eta_j + \frac{\partial F}{\partial \eta_i^2}\eta_i^2 + \sum_{j=i\pm1} \frac{\partial F}{\partial \eta_i \eta_j}\eta_i\eta_j + \ldots$$

Note, the linear terms in η_i will disappear for $i>2$ ($i=2$ second layer) for simmetry reasons. However, for the two surface planes due to the broken symmetry these terms will remain and will try to reduce the order parameter to zero at the surface. From $F/\partial\eta_i=0$ one finds thus a set of coupled Ginzburg-Landau-type equations determining η_1, η_2, etc.

REFERENCES

1. D.A. Dowden, J. Chem. Soc. 242 (1950)
2. G. Rienäcker, Abh. Deut. Akad. Wiss. Berlin, Kl. Chem. Geol. Biol. 3 (1955)
3. D.D. Eley, Z. Elektrochem., 60, 797 (1956)
4. F.F. Wolkenstein, The Electronic Theory of Catalysis, (Pergamon, Oxford, 1963)
5. J.H. Sinfelt, J.L. Carter, and D.J.C. Yates, J. Catal., 24, 283 (1972)
6. J.H. Sinfelt, J. Catal. 29, 308 (1973)
7. J. Koutecky, Prog. Surf. and Membr. Sci., 11, 1 (1976)
8. F. Cyrot-Lackmann, J. Phys. Chem. Solids, 29, 1235 (1968)
9. F. Cyrot-Lackmann, M.C. Desjonquêres and J.P. Gaspard, J. Phys. C, 7, 925 (1974)
10. R. Haydock, V. Heine, M.J. Kelly, and J.B. Pendry, Phys. Rev. Lett. 29, 868 (1972)
11. R. Haydock, V. Heine, and M.J. Kelly, J. Phys. C, 5, 2845 (1972)
12. D.M. Newns, Phys. Rev. 178, 1123 (1969)
13. T.B. Grimley and B.J. Thorpe, J. Phys. F, 1, L4 (1971)
14. J.R. Schrieffer, J. Vacuum Sci. Technol., 9,561 (1974)
15. G. Allan and P. Lenglart, J. Phys. (paris) Suppl.

C1, 93 (1970)

16. T.L. Einstein and J.R. Schrieffer, Phys. Rev. B, 7, 3625 (1973)
17. G. Doyen and G. Ertl, Surf. Sci. 43, 197 (1974)
18. At the same time our theory was published, N.F. Berk published a coherent potential approximation type theory for alloy surfaces (Surf. Sci., 48, 289 (1975)).
19. W.M.H. Sachtler and G.J.H. Dorgelo, J. Catal., 4, 654 (1965)
20. W.M.H. Sachtler, J. Vacuum Sci. Technol. 9, 828 (1972)
21. J.C. Riviere, Contem. Phys., 14, 513 (1973)
22. V. Ponec, Catal. Rev. Sci. Eng., 11, 41 (1975)
23. J.L. Beelen, V. Ponec, and W.M.H. Sachtler, J. Catal. 28, 376 (1973)
24. V.S. Sundaram, B. Farrel, R.S. Allen and W.D. Robertson, Phys. Rev. Lett. 31, 1136 (1973)
25. F. Cyrot-Lackmann, Surf. Sci., 15, 535 (1969)
26. M. Lax, Rev. Mod. Phys., 23, 287 (1951)
27. M. Lax, Phys. Rev. 85, 621 (1952)
28. S.F. Edwards, Phil. Mag., 6, 617 (1961)
29. J.L. Beeby and S.F. Edwards, Proc. Roy. Soc. (London) A274, 395 (1962)
30. J.L. Beeby, Proc. Roy. Soc. (London), A279, 82 (1964)
31. J.L. Beeby, Phys. Rev. 135, 130 (1964)
32. P. Soven, Phys. Rev. 151, 539 (1966)

33. L. Schwartz, F. Brouers, A.V. Vedyayev, and H. Ehrenreich, Phys. Rev. B, 4, 3383 (1971)

34. K.M. Watson, Phys. Rev., 105, 1388 (1957)

35. P. Soven, Phys. Rev., 156, 809 (1969)

36. B. Velický, S. Kirkpatrick and H. Ehrenreich, Phys. Rev., 175, 747 (1968)

37. P. Soven, Phys. Rev., 178, 9936 (1969)

38. S. Kirkpatrick, B. Velický and H. Ehrenreich, Phys. Rev. B, 1, 3250 (1970)

39. J.L. Morán-López, G. Kerker and K.H. Bennemann, J. Phys. F, 5, 1277 (1975)

40. N.F. Berk, Surf. Sci., 48, 289 (1975)

41. J.L. Morán-López, G. Kerker and K.H. Bennemann, Surf. Sci. 57, 540 (1976)

42. G. Kerker, J.L. Morán-López and K.H. Bennemann, Phys. Rev. B, 15, 638 (1977)

43. J.L. Morán-López, G. Kerker and K.H. Bennemann, to be published in Surf. Sci.

44. J.L. Morán-López and K.H. Bennemann, to be published.

45. J.L. Morán-López and K.H. Bennemann, Phys. Rev. B, 15, (1977)

46. R. Jacobs, J. Phys. F, 3, 933 (1973)

47. R. Jacobs, J. Phys. F, 4, 1351 (1974)

48. G.M. Stocks, R.W. Williams and J.S. Faulkner, Phys. Rev. B, 4, 4390 (1971)

49. C.D. Gelatt and H. Ehrenreich, Phys. Rev. B, 10, 398 (1974)

50. K. Levin, A. Liebsch and K.H. Bennemann, Phys. Rev. B, 7, 3066 (1973)

51. T. Yamashina, Japan J. Appl. Phys. Suppl. 2, Part 2, 493 (1974)

52. Y. Takasu and T. Yamashina, Proc. 2nd. Internl. Conf. on Solid Surfaces, Japan.

53. R.L. Moss and L. Whalley in "Advances in Catalysis" (D.D. Eley, H. Pines and P.B. Weisz. Eds) 22, p.115 Academic Press, New York, 1972.

54. J.H. Sinfelt in "Advances in Catalysis" (D.D. Eley, H.Pines and P.B. Weisz, Eds) 23, p.91, Academic Press, New York, 1973.

55. W.M.H. Sachtler and R. Jongepier, J. Catal., 4, 665, (1965)

56. R.L. Park, in "Surface Physics of Crystalline Solids", (J.M. Blakely, Ed.), Academic London, 1974.

57. F.L. Williams and D. Nason, Surf. Sci. 45, 377 (1974)

58. V.S. Sundaram and P. Wynblatt, Surf. Sci. 52, 569, (1975)

59. D. Kumar, A. Mookerjee and V. Kumar, J. Phys. F, 6, 725 (1976)

60. C.R. Helms, J. Catal. 36, 114, (1975)

61. G. Ertl and J. Küppers, Surf. Sci., 24, 104 (1971)

62. D.M. Kolb, private communication.

63. G. Doyen and G. Ertl, J. of Chem. Phys., 62, 2957 (1975)

64. J.L. Morán-López and A. ten Bosch, to be published.

65. According to Somorjai ("Principles of Surface Chemis try", Prentice Hall, New York, 1972) one obtains approximatelly $(x_A/x_B)_s=(x_A/x_B)\exp\{a(\gamma_B-\gamma_A)/kT\}$. Note, however that we find in general that $\gamma_i=\gamma_i(x)$, i=1,2.

66. R. Bouwman and W.M.H. Sachtler, J. Catal. 19, 127 (1970)

67. F.L. Williams and M. Boudart, J. Catal. 30, 438 (1973)

68. J. Friedel, Adv. Phys. 3, 446 (1954)

69. R. Defay and I. Prigogine in "Surface tension and adsorption" (Willey, New York, 1965)

70. W.L. van Dijk, J.A. Groenewegen and V. Ponec, to be published.

71. J. Giner, F. Brouers, F. Gautier and J. van der Rest, J. Phys. F, 6, 1281 (1976)

72. R.A. van Santen and W.M.H. Sachtler, J. Catal. 33, 202 (1974)

73. R.A. van Santen, L.H. Tonnemann and R. Bouwman, Surf. Sci., 47, 64 (1975)

74. E.N. Foo and H. Amar, Phys. Rev. Lett., 25, 1748 (1970)

75. M. Plischke and D. Mattis, Phys. Rev. Lett., 27, 42 (1971)

76. M. Plischke and D. Mattis, Phys. Rev. B, 7, 2430 (1973)

77. F. Brouers, J. Giner and J. Van der Rest, J. of Phys. F, 4, 214 (1974)

78. C. G. Robbins, H. Claus and P.A. Beck, Phys. Rev. Lett. 22, 1307 (1975)

José Luis Morán-López

CURRICULUM VITAE

Born 25. August 1950 in Charcas, S.L.P., Mexico.

Ground and high school in Charcas, S.L.P. 1957-1965

Continuation of the studies of high school at the Universidad Autônoma de San Luis Potosí, San Luis Potosí, S.L.P. 1966-1967.

Studies of Physics at the Escuela de Física, Universidad Autônoma de San Luis Potosí, 1968-1972.

Continuation of study towards the Master in Science degree at the Physics Department of the Centro de Investigación y de Estudios Avanzados del Instituto Politécnico Nacional, in Mexico City, 1973-1974.

Master in Science with the Thesis in the subject of Group Theory applied to Solid State Physics written under the supervision of Prof. Dr. J. Helman. August, 1974.

Assistantship at the Institute for Theoretical Physics, Freie Universität Berlin, 1974-1977.

Thesis on the subject of surface physics, written under the supervision of Prof. Dr. K.H. Bennemann, Submitted for the Doctor degree 1977.

Publications on the subject of surface physics and metal non-metal transitions.

T.O.M. DISSERTATIONSDRUCK · Lützowstr. 102 - 104 · 1000 Berlin 30 · ☎ 030 / 2 62 40 77*